

Surface induced odd-frequency spin-triplet superconductivity as a veritable signature of Majorana bound states

Subhajit Pal and Colin Benjamin*

School of Physical Sciences, National Institute of Science Education & Research, Jatni-752050, India. and Homi Bhabha National Institute, Training School Complex, AnushaktiNagar, Mumbai, 400094, India.

We predict surface-induced odd-frequency (odd- ν) spin-triplet superconducting pairing can be a veritable signature of Majorana bound states (MBS) in a Josephson nodal p -wave superconductor (p_x)-spin flipper (SF)-nodal p -wave superconductor (p_x) junction. Remarkably, in a p_x -SF- p_x Josephson junction three distinct phases emerge: the topological phase featuring MBS, the topological phase without MBS, and the trivial phase devoid of MBS. Surface odd- ν spin triplet pairing is induced only in the topological regime when MBS appear. In contrast, surface induced even-frequency (even- ν) spin triplet pairing is finite regardless of the existence of MBS. Our study offers a potential means for distinguishing the topological phase featuring MBS from both the trivial phase as well as the topological phase devoid of MBS, primarily through the observation of induced surface odd- ν spin triplet superconductivity.

I. INTRODUCTION

Odd- ν pairing is a novel superconducting state wherein the electrons in a Cooper pair have distinct time coordinates along with distinct position coordinates. Generally, two electrons in a Cooper pair are formed simultaneously, categorizing it as an even- ν pairing state[1]. Even- ν pairing state can be subdivided into two categories: even- ν spin-singlet (SS) and even- ν ST pairing states. Even- ν SS pairing is exemplified by s and d -wave pairings, while p -wave pairing serves as an illustration of even- ν ST pairing[2]. For odd- ν pairing state, Cooper pair wavefunction or pair amplitude is odd in relative time coordinate or frequency of the two Cooper pair electrons[3–5]. An odd- ν pairing state can be further categorized as odd- ν SS state and odd- ν ST state. ST states, in turn, can be classified into two subcategories: equal ST (EST) states, represented by $|\uparrow\uparrow\rangle$, $|\downarrow\downarrow\rangle$, and mixed ST (MST) states, represented by $|\uparrow\downarrow\rangle + |\downarrow\uparrow\rangle$. Odd- ν MST state was first theoretically predicted in ^3He [6]. Odd- ν EST pairing has also been theoretically predicted to occur in diffusive ferromagnet-superconductor junction where the ferromagnet has inhomogeneous magnetization[7, 8]. Earlier, it was assumed that odd- ν state was an intrinsic effect[9, 10] but later it was discovered that odd- ν state can be generated in superconducting junctions[11–30] as well as under time-dependent fields[31, 32].

Odd- ν pairing holds intrinsic significance due to its remarkable departure from conventional superconductivity. Odd- ν spin-polarized Cooper pairs exhibit resilience against both the Pauli limiting field and impurity scattering, in contrast to conventional even- ν Cooper pairs, which are only robust against impurity scattering[3]. The exceptional robustness of odd- ν pairing positions it as an attractive candidate for applications in superconducting spintronics[33].

In this work, we consider a p_x -SF- p_x Josephson junction (JJ), with the nodal p_x superconductor featuring even- ν EST pairing in its Cooper pair. Odd- ν EST pairing arises from the breaking of spatial parity[11] at the p_x - p_x interface. We see that spin-flip scattering induces odd- ν MST pairing in our setup. JJ's with p_x superconductors are theoretically predicted to harbor Majorana fermions[34]. The Majorana fermion is a particle which is its own antiparticle and has attracted a lot of attention due to its potential application in topological quantum computation[35–37]. In case of p_x -SF- p_x JJ, there is a sign change in energy bound states when Majorana fermions occur[38].

Our main motivation in this work is to distinguish MBS via the surface-induced odd- ν MST correlations in presence of spin flip scattering. Although surface odd- ν EST and surface odd- ν MST correlations are finite and large in the topological regimes when zero energy MBS occur, they vanish in their absence. Surface even- ν EST & MST correlations remain finite in both the presence and absence of MBS, rendering them ineffective for MBS detection. Surface-induced odd- ν ST correlations are a signature of MBS in p_x JJ's with a spin-flipper.

In a recent paper[39], it was seen that both odd- ν EST and even- ν EST correlations are induced in short p_x -N- p_x JJ. In Ref. [39], neither even- ν MST nor odd- ν MST correlations are present since spin flip scattering does not exist. In contrast, in our work both odd/even- ν EST and odd/even- ν MST correlations are induced via the spin flipper. In a related work[40], the authors discuss the relation between Majorana fermion and odd- ν Cooper pair in case of a disordered superconductor-metal-superconductor JJ of nanowires when the nanowire is in the topologically non-trivial regime. In the absence of spin flip scattering, it was seen that odd- ν EST pairing exists whenever MBS appear, while,

* colin.nano@gmail.com

odd- ν MST pairing does not arise. Further, the connection between MBS and odd- ν pairing has also been explored in Kitaev chain systems[41] and in spin-polarized nanowires coupled to Majorana zero modes[42, 43]. In all these Refs. [39]-[43], odd- ν MST pairing vanishes, while in our paper, due to the interplay of both MBS and spin flip scattering, odd- ν MST pairing is finite, thereby enhancing their utility in MBS detection.

The remainder of the paper is structured as follows: in the subsequent theory section, we begin by presenting the wavefunctions and boundary conditions essential for calculating bound state energies, Josephson current, and retarded Green's functions within our setup. Next, we outline the method for computing energy-bound states, retarded Green's functions, and pairing amplitudes. Moving on to Section III, we delve into the relationship between odd- ν ST superconductivity and MBS in a p_x -SF- p_x JJ. We analyze our results in the next section, offering a comparative summary of odd- and even- ν correlations induced by the presence of MBS. Finally, in section V, we summarize our work with an experimental implementation. In Appendix, we provide the analytical formulas for anomalous Green's functions, which are necessary to calculate different pairing amplitudes.

II. THEORY

A. Hamiltonian

We consider a JJ where a spin flipper (SF) is embedded between two nodal p_x superconductors, as depicted in Fig. 1. The SF's Hamiltonian is described as follows[44-48]:

$$H_{\text{SF}} = -J_0\delta(x)\vec{s} \cdot \vec{\mathcal{S}}. \quad (1)$$

We address this problem by solving a time-independent Schrödinger equation, which has been adapted to incorporate a Bogoliubov-de Gennes (BdG) Hamiltonian. The BdG Hamiltonian for p_x -SF- p_x JJ, as shown in Fig. 1, is expressed as follows:

$$H_{\text{BdG}}^{p_x\text{-SF-}p_x}(x) = \begin{pmatrix} H_P \hat{I} & \Delta_J p \hat{\sigma}_x \\ \Delta_J^* p \hat{\sigma}_x & -H_P \hat{I} \end{pmatrix}, \quad (2)$$

with $H_P = -\frac{\hbar^2}{2m^*} \frac{\partial^2}{\partial x^2} - J_0\delta(x)\vec{s} \cdot \vec{\mathcal{S}} - \mu'_{p_x}$. $-\frac{\hbar^2}{2m^*} \frac{\partial^2}{\partial x^2}$ represents electron-like quasiparticle's kinetic energy operator with an effective mass denoted as m^* , J_0 denotes the exchange interaction between the spins of the electron-like quasiparticle (\vec{s}) and SF ($\vec{\mathcal{S}}$) and, the third term corresponds to the chemical potential of a p_x -superconductor. \hat{I} represents identity matrix and $\hat{\sigma}$ being the Pauli matrices. Further, the gap parameter Δ_J has the following form $\Delta_J = \Delta'_{p_x} [e^{i\varphi_L}\theta(-x) + e^{i\varphi_R}\theta(x)]$ with Δ'_{p_x} is the pairing potential for p_x superconductor and $\theta(x)$ represents the unit step function. φ_L is the superconducting phase for left superconductor, while φ_R is the superconducting phase for right superconductor. $\varphi = \varphi_R - \varphi_L$ is the phase difference between two superconductors. In this paper, the SF's spin magnetic moment m' can have possible values, $m' = -\mathcal{S}, -\mathcal{S} + 1, \dots, \mathcal{S}$. For example, if $\mathcal{S} = 1/2$, then m' has two possible values, $m' = 1/2, -1/2$. Similarly, if $\mathcal{S} = 3/2$, then $m' = 3/2, 1/2, -1/2, -3/2$. We compute various measurable quantities like Josephson current or the pairing magnitude for each of the $2\mathcal{S} + 1$ possible values of m' for SF's spin \mathcal{S} and finally take an average over all m' values. When a spin-up electron-like quasiparticle (ELQ) interacts with the SF with a spin of $\mathcal{S} = 1/2$, it results in a product state $\frac{m'}{2} (|\uparrow\rangle_{\text{ELQ}} \otimes |\uparrow\rangle_{\text{SF}})$ if the SF's spin is in the up state ($m' = 1/2$). However, if the SF is in the spin-down state ($m' = -1/2$), an entangled state may emerge

after scattering, represented as $\left(\overbrace{\frac{f}{2} (|\downarrow\rangle_{\text{ELQ}} \otimes |\uparrow\rangle_{\text{SF}})}^{\text{Mutual spin flip}} + \overbrace{\frac{m'}{2} (|\uparrow\rangle_{\text{ELQ}} \otimes |\downarrow\rangle_{\text{SF}})}^{\text{No flip}} \right)$. In the subsequent scattering event at the SF, if a spin-down electron-like quasiparticle is incident, it encounters the SF in either the spin-up or spin-down state. If the SF is in the spin-up state, a spin flip occurs, once again leading to the formation of an entangled state. As a result, measurable quantities like Josephson current or the pairing magnitude are determined by averaging over these two processes: spin flip and no flip. This approach applies similarly to SF's spin states of $\mathcal{S} = 3/2$ and beyond, with measurable quantities calculated by averaging over all possible values of m' . In this paper, we have used dimensionless parameters $J = \frac{2m^* J_0}{k_{\mu p_x}}$ to quantify the exchange coupling strength[44], where $k_{\mu p_x} = \sqrt{\frac{2m^* \mu'_{p_x}}{\hbar^2}}$ is the Fermi momentum.

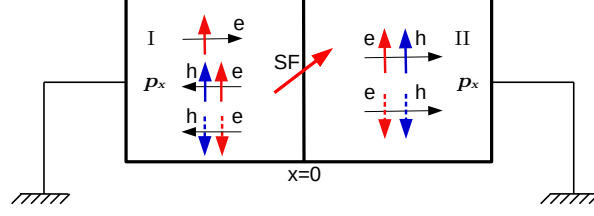


FIG. 1: Josephson junction composed of a SF at $x = 0$ embedded between two nodal p_x superconductors. Two p_x superconductors are grounded. The scattering process of an incident spin-up electron-like quasiparticle is depicted and SF's spin being oriented along any arbitrary direction.

B. Wavefunctions

By diagonalizing the Hamiltonian (2), we obtain the wavefunctions in distinct regions of the p_x -SF- p_x JJ corresponding to different scattering processes. These wavefunctions are:

$$\begin{aligned}
\Phi_1(x) &= \begin{cases} \psi_{e\uparrow}^{SL} e^{iq_e x} \phi_{m'}^S + r_{\uparrow\uparrow}^{e'e'} \psi_{e\uparrow}^{SL} e^{-iq_e x} \phi_{m'}^S + r_{\uparrow\downarrow}^{e'e'} \psi_{e\downarrow}^{SL} e^{-iq_e x} \phi_{m'+1}^S + r_{\uparrow\uparrow}^{e'h'} \psi_{h\uparrow}^{SL} e^{iq_h x} \phi_{m'}^S + r_{\uparrow\downarrow}^{e'h'} \psi_{h\downarrow}^{SL} e^{iq_h x} \phi_{m'+1}^S, & x < 0 \\ \tilde{t}_{\uparrow\uparrow}^{e'e'} \psi_{e\uparrow}^{SR} e^{iq_e x} \phi_{m'}^S + \tilde{t}_{\uparrow\downarrow}^{e'e'} \psi_{e\downarrow}^{SR} e^{iq_e x} \phi_{m'+1}^S + \tilde{t}_{\uparrow\uparrow}^{e'h'} \psi_{h\uparrow}^{SR} e^{-iq_h x} \phi_{m'}^S + \tilde{t}_{\uparrow\downarrow}^{e'h'} \psi_{h\downarrow}^{SR} e^{-iq_h x} \phi_{m'+1}^S, & x > 0 \end{cases} \\
\Phi_2(x) &= \begin{cases} \psi_{e\downarrow}^{SL} e^{iq_e x} \phi_{m'}^S + r_{\downarrow\uparrow}^{e'e'} \psi_{e\uparrow}^{SL} e^{-iq_e x} \phi_{m'-1}^S + r_{\downarrow\downarrow}^{e'e'} \psi_{e\downarrow}^{SL} e^{-iq_e x} \phi_{m'}^S + r_{\downarrow\uparrow}^{e'h'} \psi_{h\uparrow}^{SL} e^{iq_h x} \phi_{m'-1}^S + r_{\downarrow\downarrow}^{e'h'} \psi_{h\downarrow}^{SL} e^{iq_h x} \phi_{m'}^S, & x < 0 \\ \tilde{t}_{\downarrow\uparrow}^{e'e'} \psi_{e\uparrow}^{SR} e^{iq_e x} \phi_{m'-1}^S + \tilde{t}_{\downarrow\downarrow}^{e'e'} \psi_{e\downarrow}^{SR} e^{iq_e x} \phi_{m'}^S + \tilde{t}_{\downarrow\uparrow}^{e'h'} \psi_{h\uparrow}^{SR} e^{-iq_h x} \phi_{m'-1}^S + \tilde{t}_{\downarrow\downarrow}^{e'h'} \psi_{h\downarrow}^{SR} e^{-iq_h x} \phi_{m'}^S, & x > 0 \end{cases} \\
\Phi_3(x) &= \begin{cases} \psi_{h\uparrow}^{SL} e^{-iq_h x} \phi_{m'}^S + r_{\uparrow\uparrow}^{h'e'} \psi_{e\uparrow}^{SL} e^{-iq_e x} \phi_{m'}^S + r_{\uparrow\downarrow}^{h'e'} \psi_{e\downarrow}^{SL} e^{-iq_e x} \phi_{m'+1}^S + r_{\uparrow\uparrow}^{h'h'} \psi_{h\uparrow}^{SL} e^{iq_h x} \phi_{m'}^S + r_{\uparrow\downarrow}^{h'h'} \psi_{h\downarrow}^{SL} e^{iq_h x} \phi_{m'+1}^S, & x < 0 \\ \tilde{t}_{\uparrow\uparrow}^{h'e'} \psi_{e\uparrow}^{SR} e^{iq_e x} \phi_{m'}^S + \tilde{t}_{\uparrow\downarrow}^{h'e'} \psi_{e\downarrow}^{SR} e^{iq_e x} \phi_{m'+1}^S + \tilde{t}_{\uparrow\uparrow}^{h'h'} \psi_{h\uparrow}^{SR} e^{-iq_h x} \phi_{m'}^S + \tilde{t}_{\uparrow\downarrow}^{h'h'} \psi_{h\downarrow}^{SR} e^{-iq_h x} \phi_{m'+1}^S, & x > 0 \end{cases} \\
\Phi_4(x) &= \begin{cases} \psi_{h\downarrow}^{SL} e^{-iq_h x} \phi_{m'}^S + r_{\downarrow\uparrow}^{h'e'} \psi_{e\uparrow}^{SL} e^{-iq_e x} \phi_{m'-1}^S + r_{\downarrow\downarrow}^{h'e'} \psi_{e\downarrow}^{SL} e^{-iq_e x} \phi_{m'}^S + r_{\downarrow\uparrow}^{h'h'} \psi_{h\uparrow}^{SL} e^{iq_h x} \phi_{m'-1}^S + r_{\downarrow\downarrow}^{h'h'} \psi_{h\downarrow}^{SL} e^{iq_h x} \phi_{m'}^S, & x < 0 \\ \tilde{t}_{\downarrow\uparrow}^{h'e'} \psi_{e\uparrow}^{SR} e^{iq_e x} \phi_{m'-1}^S + \tilde{t}_{\downarrow\downarrow}^{h'e'} \psi_{e\downarrow}^{SR} e^{iq_e x} \phi_{m'}^S + \tilde{t}_{\downarrow\uparrow}^{h'h'} \psi_{h\uparrow}^{SR} e^{-iq_h x} \phi_{m'-1}^S + \tilde{t}_{\downarrow\downarrow}^{h'h'} \psi_{h\downarrow}^{SR} e^{-iq_h x} \phi_{m'}^S, & x > 0 \end{cases} \\
\Phi_5(x) &= \begin{cases} t_{\uparrow\uparrow}^{e'e'} \psi_{e\uparrow}^{SL} e^{-iq_e x} \phi_{m'}^S + t_{\uparrow\downarrow}^{e'e'} \psi_{e\downarrow}^{SL} e^{-iq_e x} \phi_{m'+1}^S + t_{\uparrow\uparrow}^{e'h'} \psi_{h\uparrow}^{SL} e^{iq_h x} \phi_{m'}^S + t_{\uparrow\downarrow}^{e'h'} \psi_{h\downarrow}^{SL} e^{iq_h x} \phi_{m'+1}^S, & x < 0 \\ \psi_{e\uparrow}^{SR} e^{-iq_e x} \phi_{m'}^S + \tilde{r}_{\uparrow\uparrow}^{e'e'} \psi_{e\uparrow}^{SR} e^{iq_e x} \phi_{m'}^S + \tilde{r}_{\uparrow\downarrow}^{e'e'} \psi_{e\downarrow}^{SR} e^{iq_e x} \phi_{m'+1}^S + \tilde{r}_{\uparrow\uparrow}^{e'h'} \psi_{h\uparrow}^{SR} e^{-iq_h x} \phi_{m'}^S + \tilde{r}_{\uparrow\downarrow}^{e'h'} \psi_{h\downarrow}^{SR} e^{-iq_h x} \phi_{m'+1}^S, & x > 0 \end{cases} \\
\Phi_6(x) &= \begin{cases} t_{\downarrow\uparrow}^{e'e'} \psi_{e\uparrow}^{SL} e^{-iq_e x} \phi_{m'-1}^S + t_{\downarrow\downarrow}^{e'e'} \psi_{e\downarrow}^{SL} e^{-iq_e x} \phi_{m'}^S + t_{\downarrow\uparrow}^{e'h'} \psi_{h\uparrow}^{SL} e^{iq_h x} \phi_{m'-1}^S + t_{\downarrow\downarrow}^{e'h'} \psi_{h\downarrow}^{SL} e^{iq_h x} \phi_{m'}^S, & x < 0 \\ \psi_{e\downarrow}^{SR} e^{-iq_e x} \phi_{m'}^S + \tilde{r}_{\downarrow\uparrow}^{e'e'} \psi_{e\uparrow}^{SR} e^{iq_e x} \phi_{m'-1}^S + \tilde{r}_{\downarrow\downarrow}^{e'e'} \psi_{e\downarrow}^{SR} e^{iq_e x} \phi_{m'}^S + \tilde{r}_{\downarrow\uparrow}^{e'h'} \psi_{h\uparrow}^{SR} e^{-iq_h x} \phi_{m'-1}^S + \tilde{r}_{\downarrow\downarrow}^{e'h'} \psi_{h\downarrow}^{SR} e^{-iq_h x} \phi_{m'}^S, & x > 0 \end{cases} \\
\Phi_7(x) &= \begin{cases} t_{\uparrow\uparrow}^{h'e'} \psi_{e\uparrow}^{SL} e^{-iq_e x} \phi_{m'}^S + t_{\uparrow\downarrow}^{h'e'} \psi_{e\downarrow}^{SL} e^{-iq_e x} \phi_{m'+1}^S + t_{\uparrow\uparrow}^{h'h'} \psi_{h\uparrow}^{SL} e^{iq_h x} \phi_{m'}^S + t_{\uparrow\downarrow}^{h'h'} \psi_{h\downarrow}^{SL} e^{iq_h x} \phi_{m'+1}^S, & x < 0 \\ \psi_{h\uparrow}^{SR} e^{iq_h x} \phi_{m'}^S + \tilde{r}_{\uparrow\uparrow}^{h'e'} \psi_{e\uparrow}^{SR} e^{iq_e x} \phi_{m'}^S + \tilde{r}_{\uparrow\downarrow}^{h'e'} \psi_{e\downarrow}^{SR} e^{iq_e x} \phi_{m'+1}^S + \tilde{r}_{\uparrow\uparrow}^{h'h'} \psi_{h\uparrow}^{SR} e^{-iq_h x} \phi_{m'}^S + \tilde{r}_{\uparrow\downarrow}^{h'h'} \psi_{h\downarrow}^{SR} e^{-iq_h x} \phi_{m'+1}^S, & x > 0 \end{cases} \\
\Phi_8(x) &= \begin{cases} t_{\downarrow\uparrow}^{h'e'} \psi_{e\uparrow}^{SL} e^{-iq_e x} \phi_{m'-1}^S + t_{\downarrow\downarrow}^{h'e'} \psi_{e\downarrow}^{SL} e^{-iq_e x} \phi_{m'}^S + t_{\downarrow\uparrow}^{h'h'} \psi_{h\uparrow}^{SL} e^{iq_h x} \phi_{m'-1}^S + t_{\downarrow\downarrow}^{h'h'} \psi_{h\downarrow}^{SL} e^{iq_h x} \phi_{m'}^S, & x < 0 \\ \psi_{h\downarrow}^{SR} e^{iq_h x} \phi_{m'}^S + \tilde{r}_{\downarrow\uparrow}^{h'e'} \psi_{e\uparrow}^{SR} e^{iq_e x} \phi_{m'-1}^S + \tilde{r}_{\downarrow\downarrow}^{h'e'} \psi_{e\downarrow}^{SR} e^{iq_e x} \phi_{m'}^S + \tilde{r}_{\downarrow\uparrow}^{h'h'} \psi_{h\uparrow}^{SR} e^{-iq_h x} \phi_{m'-1}^S + \tilde{r}_{\downarrow\downarrow}^{h'h'} \psi_{h\downarrow}^{SR} e^{-iq_h x} \phi_{m'}^S, & x > 0 \end{cases} \quad (3)
\end{aligned}$$

$$\begin{aligned}
\text{where } \psi_{e\uparrow}^{SL} &= \frac{1}{\sqrt{|\gamma_e|^2+1}} \begin{pmatrix} \gamma_e \\ 0 \\ 0 \\ 1 \end{pmatrix}, \psi_{e\downarrow}^{SL} = \frac{1}{\sqrt{|\gamma_e|^2+1}} \begin{pmatrix} 0 \\ \gamma_e \\ 1 \\ 0 \end{pmatrix}, \psi_{h\uparrow}^{SL} = \frac{1}{\sqrt{|\gamma_h|^2+1}} \begin{pmatrix} 0 \\ 0 \\ 0 \\ 1 \end{pmatrix}, \psi_{h\downarrow}^{SL} = \frac{1}{\sqrt{|\gamma_h|^2+1}} \begin{pmatrix} 0 \\ \gamma_h \\ 1 \\ 0 \end{pmatrix}, \psi_{e\uparrow}^{SR} = \\
&\frac{1}{\sqrt{|\gamma_e|^2+1}} \begin{pmatrix} -\gamma_e \\ 0 \\ 0 \\ 1 \end{pmatrix}, \psi_{e\downarrow}^{SR} = \frac{1}{\sqrt{|\gamma_e|^2+1}} \begin{pmatrix} 0 \\ -\gamma_e \\ 1 \\ 0 \end{pmatrix}, \psi_{h\uparrow}^{SR} = \frac{1}{\sqrt{|\gamma_h|^2+1}} \begin{pmatrix} -\gamma_h \\ 0 \\ 0 \\ 1 \end{pmatrix}, \psi_{h\downarrow}^{SR} = \frac{1}{\sqrt{|\gamma_h|^2+1}} \begin{pmatrix} 0 \\ -\gamma_h \\ 1 \\ 0 \end{pmatrix}, \psi_{e\uparrow}^{SR} = \begin{pmatrix} \gamma_e e^{i\varphi} \\ 0 \\ 0 \\ 1 \end{pmatrix}, \\
\psi_{e\downarrow}^{SR} &= \frac{1}{\sqrt{|\gamma_e|^2+1}} \begin{pmatrix} 0 \\ \gamma_e e^{i\varphi} \\ 1 \\ 0 \end{pmatrix}, \psi_{h\uparrow}^{SR} = \frac{1}{\sqrt{|\gamma_h|^2+1}} \begin{pmatrix} \gamma_h e^{i\varphi} \\ 0 \\ 0 \\ 1 \end{pmatrix}, \psi_{h\downarrow}^{SR} = \frac{1}{\sqrt{|\gamma_h|^2+1}} \begin{pmatrix} 0 \\ \gamma_h e^{i\varphi} \\ 1 \\ 0 \end{pmatrix}, \psi_{e\uparrow}^{SR} = \frac{1}{\sqrt{|\gamma_e|^2+1}} \begin{pmatrix} 0 \\ -\gamma_e e^{i\varphi} \\ 0 \\ 1 \end{pmatrix}, \psi_{e\downarrow}^{SR} = \\
&\frac{1}{\sqrt{|\gamma_e|^2+1}} \begin{pmatrix} 0 \\ -\gamma_e e^{i\varphi} \\ 1 \\ 0 \end{pmatrix}, \psi_{h\uparrow}^{SR} = \frac{1}{\sqrt{|\gamma_h|^2+1}} \begin{pmatrix} -\gamma_h e^{i\varphi} \\ 0 \\ 0 \\ 1 \end{pmatrix}, \psi_{h\downarrow}^{SR} = \frac{1}{\sqrt{|\gamma_h|^2+1}} \begin{pmatrix} 0 \\ -\gamma_h e^{i\varphi} \\ 1 \\ 0 \end{pmatrix}, \text{ and } \gamma_{e,h} = (E + q_{e,h}^2 - \mu'_{p_x}) / (\Delta'_{p_x} q_{e,h})
\end{aligned}$$

with $\hbar = 2m^* = 1$. In Eq. (3), $\Phi_1, \Phi_2, \Phi_3, \Phi_4$ denote the wavefunctions when electron-like quasiparticle with spin-up, electron-like quasiparticle with spin-down, hole-like quasiparticle with spin-up and hole-like quasiparticle with spin-down are injected from left p_x superconductor, respectively, while $\Phi_5, \Phi_6, \Phi_7, \Phi_8$ denote the wavefunctions when the corresponding quasiparticles are injected from right p_x superconductor, respectively. r_{ij}^{nn} and \tilde{r}_{ij}^{nn} are the reflection amplitudes in left p_x superconductor and right p_x superconductor respectively, while t_{ij}^{nn} and \tilde{t}_{ij}^{nn} are the transmission amplitudes in left p_x superconductor and right p_x superconductor respectively with $i, j \in \{\uparrow, \downarrow\}$ and $n \in \{e', h'\}$. The wavevectors $q_{e,h}$ in p_x superconductor can be found from

$$E^2 = (q_{e,h}^2 - \mu'_{p_x})^2 + (\Delta'_{p_x} q_{e,h})^2, \quad (\text{assuming } \hbar = 2m^* = 1). \quad (4)$$

The general solution of Eq. (4) for $q_{e,h}$ is given as,

$$q_{e,h} = \pm \sqrt{\frac{\mu'_{p_x} \pm \sqrt{E^2 + \Delta_{p_x}'^2 E^2 - \Delta_{p_x}'^2 \mu_{p_x}'^2}}{1 + \Delta_{p_x}'^2}}. \quad (5)$$

In Eq. (5), q_e and q_h have two values. The positive value of q_e (q_h) represents the electron-like (hole-like) quasiparticle moving from left (right) to right (left), while the negative value of q_e (q_h) represents the electron-like (hole-like) quasiparticle moving from right (left) to left (right). Expressions for $q_{e,h}$ for different values of chemical potential $\mu'_{p_x} \leq \Delta_{p_x}'^2/4$, $\Delta_{p_x}'^2/4 \leq \mu'_{p_x} \leq \Delta_{p_x}'^2/2$ and, $\mu'_{p_x} \geq \Delta_{p_x}'^2/2$ and energy E are provided in Table I of Ref. [49]. At $\mu'_{p_x} = 0$, the energy spectrum for p_x superconductor is gapless (see Fig. 1 of Ref. [49]) which indicates the topological transition between the trivial ($\mu'_{p_x} < 0$) and topological ($\mu'_{p_x} > 0$) phases. The gap in the energy spectrum of nodal p_x superconductor is given as

$$E_c = \begin{cases} |\mu'_{p_x}|, & \mu'_{p_x} < 0, \quad (\text{trivial regime}) \\ \mu'_{p_x}, & 0 < \mu'_{p_x} < \Delta_{p_x}'^2/2, \\ \Delta_{p_x}' \sqrt{\mu'_{p_x} - \Delta_{p_x}'^2/4}, & \mu'_{p_x} > \Delta_{p_x}'^2/2. \end{cases} \quad (\text{topological regime}) \quad (6)$$

Further, in Eq. (3), $\phi_{m'}^S$ denotes the eigenfunction of the SF, with S representing its spin and m' corresponding to its magnetic moment. The action of S^z is given as- $S^z \phi_{m'}^S = \hbar m' \phi_{m'}^S$. After diagonalizing the Hamiltonian $(H_{BdG}^{p_x\text{-SF-}p_x})^*(-k)$ instead of $H_{BdG}^{p_x\text{-SF-}p_x}(k)$, we will obtain the conjugate process $\tilde{\Phi}_i$ necessary to construct

the retarded Green's function in section II.C. For our model we notice that $\tilde{\psi}_{e\uparrow}^{SL} = \frac{1}{\sqrt{|\gamma_e|^2+1}} \begin{pmatrix} -\gamma_e \\ 0 \\ 0 \\ 1 \end{pmatrix}$, $\tilde{\psi}_{e\downarrow}^{SL} = \frac{1}{\sqrt{|\gamma_e|^2+1}} \begin{pmatrix} 0 \\ -\gamma_e \\ 1 \\ 0 \end{pmatrix}$, $\tilde{\psi}_{h\uparrow}^{SL} = \frac{1}{\sqrt{|\gamma_h|^2+1}} \begin{pmatrix} 0 \\ -\gamma_h \\ 0 \\ 1 \end{pmatrix}$, $\tilde{\psi}_{h\downarrow}^{SL} = \frac{1}{\sqrt{|\gamma_h|^2+1}} \begin{pmatrix} -\gamma_h \\ 1 \\ 0 \\ 0 \end{pmatrix}$, $\tilde{\psi}_{e\uparrow}^{SL} = \frac{1}{\sqrt{|\gamma_e|^2+1}} \begin{pmatrix} \gamma_e \\ 0 \\ 0 \\ 1 \end{pmatrix}$, $\tilde{\psi}_{e\downarrow}^{SL} = \frac{1}{\sqrt{|\gamma_e|^2+1}} \begin{pmatrix} 0 \\ \gamma_e \\ 1 \\ 0 \end{pmatrix}$, $\tilde{\psi}_{h\uparrow}^{SL} = \frac{1}{\sqrt{|\gamma_h|^2+1}} \begin{pmatrix} \gamma_h \\ 0 \\ 0 \\ 1 \end{pmatrix}$, $\tilde{\psi}_{h\downarrow}^{SL} = \frac{1}{\sqrt{|\gamma_h|^2+1}} \begin{pmatrix} 0 \\ \gamma_h \\ 1 \\ 0 \end{pmatrix}$, $\tilde{\psi}_{e\uparrow}^{SR} = \frac{1}{\sqrt{|\gamma_e|^2+1}} \begin{pmatrix} -\gamma_e e^{-i\varphi} \\ 0 \\ 0 \\ 1 \end{pmatrix}$, $\tilde{\psi}_{e\downarrow}^{SR} = \frac{1}{\sqrt{|\gamma_e|^2+1}} \begin{pmatrix} 0 \\ -\gamma_e e^{-i\varphi} \\ 1 \\ 0 \end{pmatrix}$, $\tilde{\psi}_{h\uparrow}^{SR} = \frac{1}{\sqrt{|\gamma_h|^2+1}} \begin{pmatrix} 0 \\ -\gamma_h e^{-i\varphi} \\ 0 \\ 1 \end{pmatrix}$, $\tilde{\psi}_{h\downarrow}^{SR} = \frac{1}{\sqrt{|\gamma_h|^2+1}} \begin{pmatrix} \gamma_h e^{-i\varphi} \\ 0 \\ 1 \\ 0 \end{pmatrix}$, $\tilde{\psi}_{e\uparrow}^{SR} = \frac{1}{\sqrt{|\gamma_e|^2+1}} \begin{pmatrix} \gamma_e e^{-i\varphi} \\ 0 \\ 0 \\ 1 \end{pmatrix}$, $\tilde{\psi}_{e\downarrow}^{SR} = \frac{1}{\sqrt{|\gamma_e|^2+1}} \begin{pmatrix} 0 \\ \gamma_e e^{-i\varphi} \\ 1 \\ 0 \end{pmatrix}$, $\tilde{\psi}_{h\uparrow}^{SR} = \frac{1}{\sqrt{|\gamma_h|^2+1}} \begin{pmatrix} \gamma_h e^{-i\varphi} \\ 0 \\ 0 \\ 1 \end{pmatrix}$, $\tilde{\psi}_{h\downarrow}^{SR} = \frac{1}{\sqrt{|\gamma_h|^2+1}} \begin{pmatrix} 0 \\ \gamma_h e^{-i\varphi} \\ 1 \\ 0 \end{pmatrix}$. Further, $\xi = \hbar^2/(m^* \Delta'_{p_x})$ represents the superconduct-

ing coherence length[39]. We have verified that for each kind of incident quasi-particle (electron-like/hole-like) the probability conservation $|r_{ij}^{nn}|^2 + |\tilde{t}_{ij}^{nn}|^2 = 1$ and $|\tilde{r}_{ij}^{nn}|^2 + |t_{ij}^{nn}|^2 = 1$ both below and above the gap.

C. Boundary conditions

At the p_x - p_x interface ($x = 0$), the boundary conditions are[39]:

$$\Phi_l|_{x<0} = \Phi_l|_{x>0} \quad \text{and,} \quad \frac{d\Phi_l|_{x>0}}{dx} - \frac{d\Phi_l|_{x<0}}{dx} = \frac{im^*\Delta'_{p_x}}{\hbar^2} \begin{bmatrix} 0 & (1 - e^{i\varphi})\sigma_x \\ (-1 + e^{-i\varphi})\sigma_x & 0 \end{bmatrix} \Phi_l|_{x=0} - \frac{2m^*J_0}{\hbar^2} \vec{s} \cdot \vec{\mathcal{S}} \Phi_l|_{x=0}, \quad (l = 1, 2, \dots, 8), \quad (7)$$

where $\vec{s} \cdot \vec{\mathcal{S}} = s^z \mathcal{S}^z + (s^+ \mathcal{S}^- + s^- \mathcal{S}^+)/2$ is the exchange operator of the SF's Hamiltonian[44] with $s^\pm = s_x \pm is_y$ for electron-like or hole-like quasiparticle and $\mathcal{S}^\pm = \mathcal{S}_x \pm i\mathcal{S}_y$ for the SF. For wave-functions involving electron-like quasiparticle with spin up and spin down, actions of $\vec{s} \cdot \vec{\mathcal{S}}$ are

$$\vec{s} \cdot \vec{\mathcal{S}} \psi_{e\uparrow}^S \phi_{m'}^S = \frac{\hbar^2 m'}{2} \psi_{e\uparrow}^S \phi_{m'}^S + \frac{\hbar^2 f}{2} \psi_{e\downarrow}^S \phi_{m'+1}^S, \quad \text{and,} \quad \vec{s} \cdot \vec{\mathcal{S}} \psi_{e\downarrow}^S \phi_{m'}^S = -\frac{\hbar^2 m'}{2} \psi_{e\downarrow}^S \phi_{m'}^S + \frac{\hbar^2 f'}{2} \psi_{e\uparrow}^S \phi_{m'-1}^S. \quad (8)$$

Similarly, for wave-functions involving hole-like quasiparticle with spin up and spin down, actions of $\vec{s} \cdot \vec{\mathcal{S}}$ are

$$\vec{s} \cdot \vec{\mathcal{S}} \psi_{h\uparrow}^S \phi_{m'}^S = \frac{\hbar^2 m'}{2} \psi_{h\uparrow}^S \phi_{m'}^S + \frac{\hbar^2 f}{2} \psi_{h\downarrow}^S \phi_{m'+1}^S, \quad \text{and,} \quad \vec{s} \cdot \vec{\mathcal{S}} \psi_{h\downarrow}^S \phi_{m'}^S = -\frac{\hbar^2 m'}{2} \psi_{h\downarrow}^S \phi_{m'}^S + \frac{\hbar^2 f'}{2} \psi_{h\uparrow}^S \phi_{m'-1}^S. \quad (9)$$

In Eqs. (8) and (9), $f = \sqrt{(\mathcal{S} - m')(\mathcal{S} + m' + 1)}$ represents the probability of spin flip for the incident process of a spin-up electron-like or hole-like quasiparticle, where $f' = \sqrt{(\mathcal{S} + m')(\mathcal{S} - m' + 1)}$ represents the probability of spin flip for the incident process of a spin-down electron-like or hole-like quasiparticle. By employing the equations above and solving the boundary condition (Eq. (7)), we obtain a set of eight equations for scattering processes, as shown in Eq. (3). Various scattering amplitudes r_{ij}^{nn} , \tilde{r}_{ij}^{nn} , \tilde{t}_{ij}^{nn} , t_{ij}^{nn} for each kind of incident quasiparticle (electron-like/hole-like) are determined from these 8 equations. We have verified the detailed balance condition[50] for Andreev reflection, i.e., $\frac{r_{ij}^{e'h'}(-\varphi, \nu)}{q_e} = \frac{r_{ij}^{h'e'}(\varphi, \nu)}{q_h}$ and, $\frac{\tilde{r}_{ij}^{e'h'}(-\varphi, \nu)}{q_e} = \frac{\tilde{r}_{ij}^{h'e'}(\varphi, \nu)}{q_h}$, which implies the accuracy of our calculation. In the subsequent sections, we will employ normalized pairing potential, denoted as $\Delta_{p_x} = \frac{2m^*\Delta'_{p_x}}{\hbar^2 k_{\mu p_x}}$, and normalized chemical potential, denoted as $\mu_{p_x} = \frac{\hbar^2 \mu'_{p_x}}{m^* \Delta_{p_x}^2}$.

D. Bound state energies

To compute energy bound states in p_x -SF- p_x JJ we neglect the contribution from incoming quasiparticles in the wavefunctions[51, 52], see Eq. (3) and substitute these wavefunctions into the boundary conditions, see Eq. (7). We will get 8 equations, with

$$Py = 0, \quad (10)$$

and wherein $y = [r_{\uparrow\uparrow}^{e'e'}, r_{\uparrow\downarrow}^{e'e'}, r_{\uparrow\uparrow}^{e'h'}, r_{\uparrow\downarrow}^{e'h'}, \tilde{t}_{\uparrow\uparrow}^{e'e'}, \tilde{t}_{\uparrow\downarrow}^{e'e'}, \tilde{t}_{\uparrow\uparrow}^{e'h'}, \tilde{t}_{\uparrow\downarrow}^{e'h'}]^T$ is a 8×1 column matrix and P is a 8×8 matrix. For nontrivial solution of Eq. (10), the det P should be zero and we obtain bound state energies $E_l (l = 1, \dots, 8) = \pm E_n (n = 1, \dots, 4)$. Since we consider a short JJ, the Josephson total current is equal to the Josephson bound current, which can be obtained from bound state energies[53],

$$I = -\frac{2e}{\hbar} \sum_{n=1}^4 \tanh\left(\frac{E_n}{2k_B T}\right) \frac{dE_n}{d\varphi}, \quad (11)$$

E. Green's functions

The primary objective of this study is to investigate the potential correlation between the presence of MBS and the emergence of odd- ν pairing correlations. For this reason, we form retarded Green's function, denoted as $\mathcal{G}^r(x, \bar{x}, \nu)$, for the setup depicted in Fig. 1, incorporating the interface scattering processes[54]. Following Refs. [55] and [56],

$\mathcal{G}^r(x, \bar{x}, \nu)$ can be expressed as-

$$\mathcal{G}^r(x, \bar{x}, \nu) = \begin{cases} \Phi_1(x)[\alpha_{11}\tilde{\Phi}_5^T(\bar{x}) + \alpha_{12}\tilde{\Phi}_6^T(\bar{x}) + \alpha_{13}\tilde{\Phi}_7^T(\bar{x}) + \alpha_{14}\tilde{\Phi}_8^T(\bar{x})] \\ + \Phi_2(x)[\alpha_{21}\tilde{\Phi}_5^T(\bar{x}) + \alpha_{22}\tilde{\Phi}_6^T(\bar{x}) + \alpha_{23}\tilde{\Phi}_7^T(\bar{x}) + \alpha_{24}\tilde{\Phi}_8^T(\bar{x})] \\ + \Phi_3(x)[\alpha_{31}\tilde{\Phi}_5^T(\bar{x}) + \alpha_{32}\tilde{\Phi}_6^T(\bar{x}) + \alpha_{33}\tilde{\Phi}_7^T(\bar{x}) + \alpha_{34}\tilde{\Phi}_8^T(\bar{x})] \\ + \Phi_4(x)[\alpha_{41}\tilde{\Phi}_5^T(\bar{x}) + \alpha_{42}\tilde{\Phi}_6^T(\bar{x}) + \alpha_{43}\tilde{\Phi}_7^T(\bar{x}) + \alpha_{44}\tilde{\Phi}_8^T(\bar{x})], & x > \bar{x} \\ \Phi_5(x)[\beta_{11}\tilde{\Phi}_1^T(\bar{x}) + \beta_{12}\tilde{\Phi}_2^T(\bar{x}) + \beta_{13}\tilde{\Phi}_3^T(\bar{x}) + \beta_{14}\tilde{\Phi}_4^T(\bar{x})] \\ + \Phi_6(x)[\beta_{21}\tilde{\Phi}_1^T(\bar{x}) + \beta_{22}\tilde{\Phi}_2^T(\bar{x}) + \beta_{23}\tilde{\Phi}_3^T(\bar{x}) + \beta_{24}\tilde{\Phi}_4^T(\bar{x})] \\ + \Phi_7(x)[\beta_{31}\tilde{\Phi}_1^T(\bar{x}) + \beta_{32}\tilde{\Phi}_2^T(\bar{x}) + \beta_{33}\tilde{\Phi}_3^T(\bar{x}) + \beta_{34}\tilde{\Phi}_4^T(\bar{x})] \\ + \Phi_8(x)[\beta_{41}\tilde{\Phi}_1^T(\bar{x}) + \beta_{42}\tilde{\Phi}_2^T(\bar{x}) + \beta_{43}\tilde{\Phi}_3^T(\bar{x}) + \beta_{44}\tilde{\Phi}_4^T(\bar{x})], & x < \bar{x}. \end{cases} \quad (12)$$

In Eq. (12), α_{ij} and β_{mn} ($i, j \in 1, \dots, 4$ and $m, n \in 1, \dots, 4$) are determined from the equation of motion of the Green's function,

$$[\nu - H_{BdG}^{p_x\text{-SF-}p_x}(x)]\mathcal{G}^r(x, \bar{x}, \nu) = \delta(x - \bar{x}). \quad (13)$$

If we integrate Eq. (13) with respect to x over the vicinity of $x = \bar{x}$, we get,

$$[\mathcal{G}^r(x > \bar{x})]_{x=\bar{x}} = [\mathcal{G}^r(x < \bar{x})]_{x=\bar{x}}, \quad \left[\frac{d}{dx}\mathcal{G}^r(x > \bar{x})\right]_{x=\bar{x}} - \left[\frac{d}{dx}\mathcal{G}^r(x < \bar{x})\right]_{x=\bar{x}} = \eta\tau_z\sigma_0, \quad (14)$$

where $\eta = \frac{2m^*}{\hbar^2}$. \mathcal{G}^r is represented as,

$$\mathcal{G}^r(x, \bar{x}, \nu) = \begin{bmatrix} \mathcal{G}_{ee}^r & \mathcal{G}_{eh}^r \\ \mathcal{G}_{he}^r & \mathcal{G}_{hh}^r \end{bmatrix}, \quad (15)$$

where \mathcal{G}_{ee}^r , \mathcal{G}_{eh}^r , \mathcal{G}_{he}^r , \mathcal{G}_{hh}^r are matrices. The anomalous component of the \mathcal{G}^r , necessary for calculating pairing amplitudes when spin flip scattering is considered, is given by

$$\mathcal{G}_{eh}^r = \begin{bmatrix} [\mathcal{G}_{eh}^r]_{\uparrow\downarrow} & [\mathcal{G}_{eh}^r]_{\uparrow\uparrow} \\ [\mathcal{G}_{eh}^r]_{\downarrow\downarrow} & [\mathcal{G}_{eh}^r]_{\downarrow\uparrow} \end{bmatrix}. \quad (16)$$

Next, we calculate pairing amplitudes from anomalous component of \mathcal{G}^r .

1. Pairing amplitudes

Anomalous component of $\mathcal{G}^r(x, \bar{x}, \nu)$ is expressed as,

$$\mathcal{G}_{eh}^r(x, \bar{x}, \nu) = i \sum_{l=0}^3 f_l^r \sigma_l \sigma_2. \quad (17)$$

In Eq. (17), σ_0 represents the Identity matrix and, σ_l ($l = 1, 2, 3$) denote the Pauli matrices. Further, f_0^r is spin-singlet ($\uparrow\downarrow - \downarrow\uparrow$) pairing amplitude, $f_{1,2}^r$ represent equal spin-triplet ($\downarrow\downarrow \pm \uparrow\uparrow$) pairing amplitudes and finally f_3^r being the mixed spin-triplet ($\uparrow\downarrow + \downarrow\uparrow$) pairing amplitude. The EST pairing amplitudes $\uparrow\uparrow$ and $\downarrow\downarrow$ are calculated as $f_{\uparrow\uparrow}^r = if_2^r - f_1^r$ and $f_{\downarrow\downarrow}^r = if_2^r + f_1^r$, respectively. Even and odd- ν pairing amplitudes are obtained from,

$$f_l^E(x, \bar{x}, \nu) = \frac{f_l^r(x, \bar{x}, \nu) + f_l^a(x, \bar{x}, -\nu)}{2}, \quad \text{and} \quad f_l^O(x, \bar{x}, \nu) = \frac{f_l^r(x, \bar{x}, \nu) - f_l^a(x, \bar{x}, -\nu)}{2}, \quad (18)$$

f_l^a are the advanced Green's function and determined from $\mathcal{G}^a(x, \bar{x}, \nu) = [\mathcal{G}^r(\bar{x}, x, \nu)]^\dagger$ [55]. The even and odd- ν EST pairing amplitudes are calculated as,

$$\text{Even-}\nu \text{ EST: } f_{\uparrow\uparrow}^E = if_2^E - f_1^E \quad \text{and} \quad f_{\downarrow\downarrow}^E = if_2^E + f_1^E; \quad \text{Odd-}\nu \text{ EST: } f_{\uparrow\uparrow}^O = if_2^O - f_1^O \quad \text{and} \quad f_{\downarrow\downarrow}^O = if_2^O + f_1^O. \quad (19)$$

The even and odd- ν MST pairing amplitudes are calculated as,

$$\text{Even-}\nu \text{ MST: } f_3^E(x, \bar{x}, \nu) = \frac{f_3^r(x, \bar{x}, \nu) + f_3^a(x, \bar{x}, -\nu)}{2}; \quad \text{Odd-}\nu \text{ MST: } f_3^O(x, \bar{x}, \nu) = \frac{f_3^r(x, \bar{x}, \nu) - f_3^a(x, \bar{x}, -\nu)}{2}. \quad (20)$$

In Appendix, analytical formulas for the anomalous Green's functions are provided.

III. RESULTS

A. Majorana bound states and Josephson current

We calculate energy-bound states and Josephson current using the method as outlined in section II.D. In Figs. 2(a), (b), bound state energies are plotted as a function of phase difference φ in both topological (Fig. 2(a)) and trivial (Fig. 2(b)) regimes. From Fig. 2(a), we see that in the topological regime at $\varphi = \pm\pi$, energy bound states change their sign due to their 4π periodicity, which indicates the presence of Majorana zero modes inside the junction[38]. This 4π periodic energy bound states occur because of the coupling of two Majorana fermions at zero energy. However, in the trivial regime energy bound states do not change their sign, see Fig. 2(b), and they are 2π periodic, which indicates the absence of MBS. In Fig. 2(c), we plot Josephson current versus phase difference (φ) for both topological and trivial regimes. We notice that in the topological regime, Josephson current is also 4π periodic and becomes maximum at $\varphi = \pi$ when MBS occur. However, Josephson current is 2π periodic and vanishes at $\varphi = \pm\pi$ in the trivial regime when MBS do not occur.

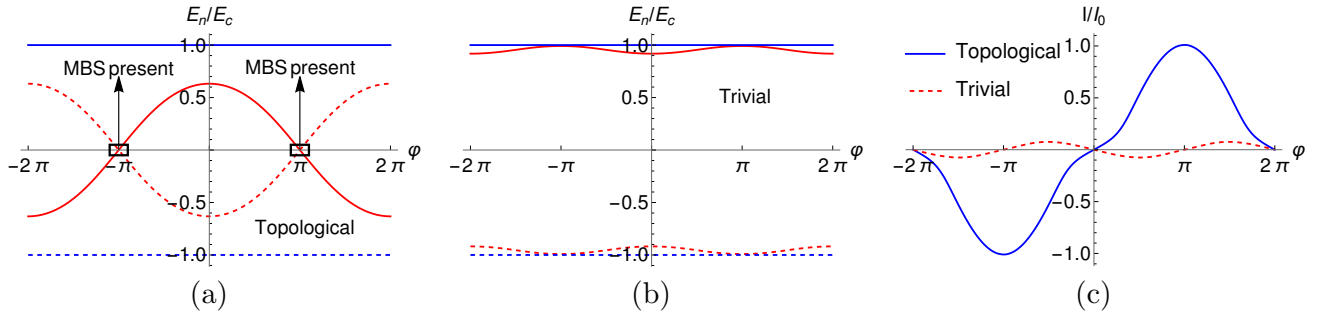


FIG. 2: Energy bound states as function of phase difference φ for (a) topological regime, (b) trivial regime. (c) Josephson current as a function of phase difference φ . Parameters: $S = 1/2$, $J = 3$, $\mu_{p_x} = 1$ (for topological regime), $\mu_{p_x} = -1$ (for trivial regime), $\Delta_{p_x} = \sqrt{2}$, $E_c = 1$, $I_0 = eE_c/\hbar$, $T = 0$. In (a) and (b) we choose the particular case of $S = -m' = 1/2$.

B. Odd-frequency pairing and Majorana bound states

1. Equal spin-triplet (EST) superconducting correlations

We calculate even- and odd- ν pairing amplitudes using Eqs. (17), (18), (19) and, (20). Spin-singlet (SS) pairing is zero in the setup considered in Fig. 1, however spin-triplet (ST) pairing is finite. ST pairing is of two kinds, equal spin-triplet (EST) pairing and mixed spin-triplet (MST) pairing. Since, in our work, p_x superconductor has equal spin-triplet Cooper pair, thus EST pairing already exists in this setup, however, MST pairing is induced due to the spin flipper. Here we show that even- ν EST and odd- ν EST pairings are induced in our setup due to the p_x superconductor. Similar to Fig. 2, we look at two cases: (a) the trivial regime and, (b) the topological regime. In the **trivial** regime, both bulk and surface even- ν EST pairing are non-zero in the left superconductor and given as:

$$\begin{aligned} \text{Bulk even-}\nu \text{ EST: } f_{\uparrow\uparrow}^{E,B}(x, \bar{x}, \nu) &= \frac{i\eta}{8(q_h\gamma_e - q_e\gamma_h)} \left(4\gamma_e\gamma_h (e^{-iq_h|x-\bar{x}|} - e^{iq_e|x-\bar{x}|}) \text{sgn}(x - \bar{x}) \right) \\ &= f_{\downarrow\downarrow}^{E,B}(x, \bar{x}, \nu), \text{ for } x < 0, \end{aligned} \quad (21)$$

$$\begin{aligned} \text{Surface even-}\nu \text{ EST: } f_{\uparrow\uparrow}^{E,S}(x, \bar{x}, \nu) &= \frac{i\eta}{8(q_h\gamma_e - q_e\gamma_h)} \left((\gamma_h^2 \sqrt{\frac{1-\gamma_e^2}{1-\gamma_h^2}} (r_{\uparrow\uparrow}^{e'h'} + r_{\downarrow\downarrow}^{e'h'}) + \gamma_e^2 \sqrt{\frac{1-\gamma_h^2}{1-\gamma_e^2}} (r_{\uparrow\uparrow}^{h'e'} + r_{\downarrow\downarrow}^{h'e'})) \right) \\ &\times (e^{-i(q_e x - q_h \bar{x})} - e^{-i(q_e \bar{x} - q_h x)}) = f_{\downarrow\downarrow}^{E,S}(x, \bar{x}, \nu), \text{ for } x < 0, \end{aligned} \quad (22)$$

while bulk odd- ν EST pairing vanishes even though surface odd- ν EST pairing is non-zero, and given as,

$$\text{Bulk odd-}\nu \text{ EST: } f_{\uparrow\uparrow}^{O,B}(x, \bar{x}, \nu) = 0 = f_{\downarrow\downarrow}^{O,B}(x, \bar{x}, \nu), \text{ for } x < 0, \quad (23)$$

$$\begin{aligned} \text{Surface odd-}\nu \text{ EST: } f_{\uparrow\uparrow}^{O,S}(x, \bar{x}, \nu) &= -\frac{i\eta}{8(q_h\gamma_e - q_e\gamma_h)} \left(2\gamma_e\gamma_h((r_{\uparrow\uparrow}^{e'e'} + r_{\downarrow\downarrow}^{e'e'})e^{-iq_e(x+\bar{x})} - (r_{\uparrow\uparrow}^{h'h'} + r_{\downarrow\downarrow}^{h'h'})e^{iq_h(x+\bar{x})}) \right) \\ &+ \left(-\gamma_h^2\sqrt{\frac{1-\gamma_e^2}{1-\gamma_h^2}}(r_{\uparrow\uparrow}^{e'h'} + r_{\downarrow\downarrow}^{e'h'}) + \gamma_e^2\sqrt{\frac{1-\gamma_h^2}{1-\gamma_e^2}}(r_{\uparrow\uparrow}^{h'e'} + r_{\downarrow\downarrow}^{h'e'}) \right) (e^{i(q_hx - q_e\bar{x})} + e^{i(q_h\bar{x} - q_ex)}) \\ &= f_{\downarrow\downarrow}^{O,S}(x, \bar{x}, \nu), \text{ for } x < 0. \end{aligned} \quad (24)$$

However, in the **topological** regime, both bulk and surface even- ν EST pairing are non-zero in the left superconductor and given as:

$$\begin{aligned} \text{Bulk even-}\nu \text{ EST: } f_{\uparrow\uparrow}^{E,B}(x, \bar{x}, \nu) &= \frac{i\eta}{8(q_e\gamma_e - q_h\gamma_h)} \left(2(e^{-iq_h|x-\bar{x}|} - e^{iq_e|x-\bar{x}|})\text{sgn}(x - \bar{x}) \right) + \frac{i\eta}{8(q_h\gamma_e - q_e\gamma_h)} \\ &\times \left(2\gamma_e\gamma_h(e^{-iq_h|x-\bar{x}|} - e^{iq_e|x-\bar{x}|})\text{sgn}(x - \bar{x}) \right) = f_{\downarrow\downarrow}^{E,B}(x, \bar{x}, \nu), \text{ for } x < 0, \end{aligned} \quad (25)$$

$$\begin{aligned} \text{Surface even-}\nu \text{ EST: } f_{\uparrow\uparrow}^{E,S}(x, \bar{x}, \nu) &= \frac{i\eta}{8(q_e\gamma_e - q_h\gamma_h)} \left((r_{\uparrow\uparrow}^{e'h'^*} + r_{\downarrow\downarrow}^{e'h'^*})e^{-i(q_ex - q_h\bar{x})} - (r_{\uparrow\uparrow}^{h'e'^*} + r_{\downarrow\downarrow}^{h'e'^*})e^{i(q_hx - q_e\bar{x})} \right) \\ &+ \frac{i\eta}{8(q_h\gamma_e - q_e\gamma_h)} \left(-\gamma_h^2(r_{\uparrow\uparrow}^{e'h'} + r_{\downarrow\downarrow}^{e'h'})e^{-i(q_e\bar{x} - q_hx)} + \gamma_e^2(r_{\uparrow\uparrow}^{h'e'} + r_{\downarrow\downarrow}^{h'e'})e^{-i(q_ex - q_h\bar{x})} \right) \\ &= f_{\downarrow\downarrow}^{E,S}(x, \bar{x}, \nu), \text{ for } x < 0. \end{aligned} \quad (26)$$

But in contrast to trivial regime wherein bulk odd- ν EST pairing vanishes, in topological regime both bulk odd- ν EST pairing and surface odd- ν EST pairing are non-zero, and given by-

$$\begin{aligned} \text{Bulk odd-}\nu \text{ EST: } f_{\uparrow\uparrow}^{O,B}(x, \bar{x}, \nu) &= \frac{i\eta}{8(q_e\gamma_e - q_h\gamma_h)} \left(-2(e^{-iq_h|x-\bar{x}|} - e^{iq_e|x-\bar{x}|})\text{sgn}(x - \bar{x}) \right) + \frac{i\eta}{8(q_h\gamma_e - q_e\gamma_h)} \\ &\times \left(2\gamma_e\gamma_h(e^{-iq_h|x-\bar{x}|} - e^{iq_e|x-\bar{x}|})\text{sgn}(x - \bar{x}) \right) = f_{\downarrow\downarrow}^{O,B}(x, \bar{x}, \nu), \text{ for } x < 0, \end{aligned} \quad (27)$$

$$\begin{aligned} \text{Surface odd-}\nu \text{ EST: } f_{\uparrow\uparrow}^{O,S}(x, \bar{x}, \nu) &= \frac{i\eta}{8(q_e\gamma_e - q_h\gamma_h)} \left((r_{\uparrow\uparrow}^{e'e'} + r_{\downarrow\downarrow}^{e'e'})e^{-iq_e(x+\bar{x})} - (r_{\uparrow\uparrow}^{h'h'} + r_{\downarrow\downarrow}^{h'h'})e^{iq_h(x+\bar{x})} - (r_{\uparrow\uparrow}^{e'h'^*} + r_{\downarrow\downarrow}^{e'h'^*}) \right) \\ &\times e^{-i(q_ex - q_h\bar{x})} + (r_{\uparrow\uparrow}^{h'e'^*} + r_{\downarrow\downarrow}^{h'e'^*})e^{i(q_hx - q_e\bar{x})} \left. + \frac{i\eta}{8(q_h\gamma_e - q_e\gamma_h)} \left(\gamma_e\gamma_h(r_{\uparrow\uparrow}^{e'e'} + r_{\downarrow\downarrow}^{e'e'}) \right) \right) \\ &\times e^{-iq_e(x+\bar{x})} - \gamma_e\gamma_h(r_{\uparrow\uparrow}^{h'h'} + r_{\downarrow\downarrow}^{h'h'})e^{iq_h(x+\bar{x})} - \gamma_h^2(r_{\uparrow\uparrow}^{e'h'} + r_{\downarrow\downarrow}^{e'h'})e^{-i(q_e\bar{x} - q_hx)} \\ &+ \gamma_e^2(r_{\uparrow\uparrow}^{h'e'} + r_{\downarrow\downarrow}^{h'e'})e^{-i(q_ex - q_h\bar{x})} \left. = f_{\downarrow\downarrow}^{O,S}(x, \bar{x}, \nu), \text{ for } x < 0. \right) \end{aligned} \quad (28)$$

In the above equations, we have separated the pairing amplitudes into bulk (B) and surface (S) components, where bulk components do not depend on interface scattering amplitudes. From Eqs. (21)-(24), we notice that in the trivial regime even- ν EST correlations survive both in bulk and surface, while odd- ν EST correlations exist only in surface. In the topological regime, both even- ν EST and odd- ν EST correlations exist in bulk as well as in surface as seen from Eqs. (25)-(28).

1.1 Zero frequency limit of EST correlations

In the topological regime, MBS appear at $\nu \rightarrow 0$ and $\varphi = \pm\pi$ as depicted in Fig. 2(a). To understand the nature of even- ν EST and odd- ν EST correlations when MBS appear in the topological regime, we look at the $\nu \rightarrow 0$ limit in both trivial and topological regimes. In the **trivial** regime, for $\nu \rightarrow 0$, $\gamma_e \approx \gamma_h \approx I$, $r_{\uparrow\uparrow}^{e'e'} = r_{\downarrow\downarrow}^{e'e'} = r_{\uparrow\uparrow}^{h'h'} = r_{\downarrow\downarrow}^{h'h'} = 0$, $r_{\uparrow\uparrow}^{e'h'} = r_{\uparrow\uparrow}^{h'e'}$ and, $r_{\downarrow\downarrow}^{e'h'} = r_{\downarrow\downarrow}^{h'e'}$. We should mention that the Andreev reflection amplitudes $r_{\uparrow\uparrow}^{e'h'}$, $r_{\uparrow\uparrow}^{h'e'}$, $r_{\downarrow\downarrow}^{e'h'}$, $r_{\downarrow\downarrow}^{h'e'}$ are purely real and its because of the perfect Andreev reflection seen at $\nu \rightarrow 0$ limit. From Eqs. (21)-(24) we get, in

$\nu \rightarrow 0$ limit,

$$\text{Bulk even-}\nu \text{ EST: } f_{\uparrow\uparrow}^{E,B}(x, \bar{x}, \nu \rightarrow 0) = \frac{\eta}{2(q_h - q_e)} \left((e^{iq_e|x-\bar{x}|} - e^{-iq_h|x-\bar{x}|}) \text{sgn}(x - \bar{x}) \right) = f_{\downarrow\downarrow}^{E,B}(x, \bar{x}, \nu \rightarrow 0),$$

for $x < 0$,

(29)

$$\text{Surface even-}\nu \text{ EST: } f_{\uparrow\uparrow}^{E,S}(x, \bar{x}, \nu \rightarrow 0) = \frac{\eta}{4(q_h - q_e)} \left((r_{\uparrow\uparrow}^{e'h'} + r_{\downarrow\downarrow}^{e'h'}) (e^{-i(q_e\bar{x}-q_hx)} - e^{-i(q_ex-q_h\bar{x})}) \right) = f_{\downarrow\downarrow}^{E,S}(x, \bar{x}, \nu \rightarrow 0),$$

for $x < 0$,

(30)

$$\text{Bulk odd-}\nu \text{ EST: } f_{\uparrow\uparrow}^{O,B}(x, \bar{x}, \nu \rightarrow 0) = 0 = f_{\downarrow\downarrow}^{O,B}(x, \bar{x}, \nu \rightarrow 0), \text{ for } x < 0,$$
(31)

$$\text{Surface odd-}\nu \text{ EST: } f_{\uparrow\uparrow}^{O,S}(x, \bar{x}, \nu \rightarrow 0) = 0 = f_{\downarrow\downarrow}^{O,S}(x, \bar{x}, \nu \rightarrow 0), \text{ for } x < 0.$$
(32)

Thus, in trivial regime at $\nu \rightarrow 0$ limit odd- ν EST pairing vanishes. In the **topological** regime, at $\nu \rightarrow 0$, $\gamma_h \approx -\gamma_e$, $(q_e\gamma_e - q_h\gamma_h)\gamma_e^2 + (q_h\gamma_e - q_e\gamma_h) \ll 1$, $r_{\uparrow\uparrow}^{e'e'} = r_{\uparrow\uparrow}^{h'h'}$, $r_{\downarrow\downarrow}^{e'e'} = r_{\downarrow\downarrow}^{h'h'}$ and with MBS are **absent** ($\varphi \neq \pi$), normal reflection amplitudes $r_{\uparrow\uparrow}^{e'e'} = r_{\downarrow\downarrow}^{e'e'} = r_{\uparrow\uparrow}^{h'h'} = r_{\downarrow\downarrow}^{h'h'} = 0$ and, Andreev reflection amplitudes, $r_{\uparrow\uparrow}^{e'h'} = r_{\downarrow\downarrow}^{e'h'} = r_{\uparrow\uparrow}^{h'e'} = r_{\downarrow\downarrow}^{h'e'}$ (all are imaginary), thus from Eqs. (25)-(28) we get,

$$\text{Bulk even-}\nu \text{ EST: } f_{\uparrow\uparrow}^{E,B}(x, \bar{x}, \nu \rightarrow 0) = \frac{i\eta}{2\gamma_e(q_e + q_h)} \left((e^{-iq_h|x-\bar{x}|} - e^{iq_e|x-\bar{x}|}) \text{sgn}(x - \bar{x}) \right) = f_{\downarrow\downarrow}^{E,B}(x, \bar{x}, \nu \rightarrow 0),$$

for $x < 0$,

(33)

$$\text{Surface even-}\nu \text{ EST: } f_{\uparrow\uparrow}^{E,S}(x, \bar{x}, \nu \rightarrow 0) = \frac{i\eta}{2\gamma_e(q_e + q_h)} \left(r_{\uparrow\uparrow}^{e'h'} (e^{-i(q_e\bar{x}-q_hx)} - e^{-i(q_ex-q_h\bar{x})}) \right) = f_{\downarrow\downarrow}^{E,S}(x, \bar{x}, \nu \rightarrow 0),$$

for $x < 0$,

(34)

$$\text{Bulk odd-}\nu \text{ EST: } f_{\uparrow\uparrow}^{O,B}(x, \bar{x}, \nu \rightarrow 0) = 0 = f_{\downarrow\downarrow}^{O,B}(x, \bar{x}, \nu \rightarrow 0), \text{ for } x < 0,$$
(35)

$$\text{Surface odd-}\nu \text{ EST: } f_{\uparrow\uparrow}^{O,S}(x, \bar{x}, \nu \rightarrow 0) = 0 = f_{\downarrow\downarrow}^{O,S}(x, \bar{x}, \nu \rightarrow 0), \text{ for } x < 0.$$
(36)

Again in topological regime at $\nu \rightarrow 0$ limit odd- ν EST pairing vanishes when MBS are absent. Further, in the **topological** regime, when MBS are **present** ($\varphi = \pi$), normal reflection amplitudes satisfy $r_{\uparrow\uparrow}^{e'e'} = r_{\uparrow\uparrow}^{h'h'}$, $r_{\downarrow\downarrow}^{e'e'} = r_{\downarrow\downarrow}^{h'h'}$ and, Andreev reflection amplitudes satisfy $r_{\uparrow\uparrow}^{e'h'} = r_{\uparrow\uparrow}^{h'e'}$, $r_{\downarrow\downarrow}^{e'h'} = r_{\downarrow\downarrow}^{h'e'}$ with $\text{Im}[r_{\uparrow\uparrow}^{e'h'}] \gg 1$, $\text{Im}[r_{\downarrow\downarrow}^{e'h'}] \gg 1$, thus from Eqs. (25)-(28) we get,

$$\text{Bulk even-}\nu \text{ EST: } f_{\uparrow\uparrow}^{E,B}(x, \bar{x}, \nu \rightarrow 0) = \frac{i\eta}{2\gamma_e(q_e + q_h)} \left((e^{-iq_h|x-\bar{x}|} - e^{iq_e|x-\bar{x}|}) \text{sgn}(x - \bar{x}) \right) = f_{\downarrow\downarrow}^{E,B}(x, \bar{x}, \nu \rightarrow 0),$$

for $x < 0$,

(37)

$$\text{Surface even-}\nu \text{ EST: } f_{\uparrow\uparrow}^{E,S}(x, \bar{x}, \nu \rightarrow 0) = \frac{i\eta}{8\gamma_e(q_e + q_h)} \left((r_{\uparrow\uparrow}^{h'e'} + r_{\downarrow\downarrow}^{h'e'}) (1 + \gamma_e^2) e^{-i(q_ex-q_h\bar{x})} - (r_{\uparrow\uparrow}^{e'h'} + r_{\downarrow\downarrow}^{e'h'}) (1 + \gamma_h^2) \right. \\ \left. \times e^{i(q_hx-q_e\bar{x})} \right) = f_{\downarrow\downarrow}^{E,S}(x, \bar{x}, \nu \rightarrow 0), \text{ for } x < 0,$$
(38)

$$\text{Bulk odd-}\nu \text{ EST: } f_{\uparrow\uparrow}^{O,B}(x, \bar{x}, \nu \rightarrow 0) = 0 = f_{\downarrow\downarrow}^{O,B}(x, \bar{x}, \nu \rightarrow 0), \text{ for } x < 0,$$
(39)

$$\text{Surface odd-}\nu \text{ EST: } f_{\uparrow\uparrow}^{O,S}(x, \bar{x}, \nu \rightarrow 0) = \frac{i\eta}{8\gamma_e(q_e + q_h)} \left(2(r_{\uparrow\uparrow}^{e'e'} + r_{\downarrow\downarrow}^{e'e'}) e^{-iq_e(x+\bar{x})} - 2(r_{\uparrow\uparrow}^{h'h'} + r_{\downarrow\downarrow}^{h'h'}) e^{iq_h(x+\bar{x})} - (r_{\uparrow\uparrow}^{h'e'} \right. \\ \left. + r_{\downarrow\downarrow}^{h'e'}) \times (1 - \gamma_e^2) e^{-i(q_ex-q_h\bar{x})} + (r_{\uparrow\uparrow}^{e'h'} + r_{\downarrow\downarrow}^{e'h'}) (1 - \gamma_h^2) e^{i(q_hx-q_e\bar{x})} \right) \\ = f_{\downarrow\downarrow}^{O,S}(x, \bar{x}, \nu \rightarrow 0), \text{ for } x < 0.$$
(40)

In topological regime at $\nu \rightarrow 0$ limit, surface odd- ν EST correlations are finite when MBS are present. This can act as a signature of MBS. From Eqs. (29)-(40), we see that both bulk and surface contribution of odd- ν EST correlations vanish in the trivial regime and in the topological regime when MBS are absent at $\nu \rightarrow 0$ limit, while only bulk contribution of odd- ν EST correlations vanish in the topological regime when MBS are present. Bulk and surface contributions of Even- ν EST and odd- ν EST correlations at $\nu \rightarrow 0$ within the left superconductor are presented in Fig. 3. We choose three cases: (a) trivial regime, (b) topological regime when MBS are absent, and (c) topological regime when MBS are present. From Fig. 3, it is evident that, in the trivial regime both bulk and surface contributions of even- ν EST correlations are finite and exhibit a decay without any oscillation with vanishing odd- ν EST correlations. However, in the topological regime when MBS are absent, both bulk and surface contributions

of even- ν EST correlations are nonzero and exhibit an oscillatory decay with vanishing odd- ν EST correlations. In the topological regime, when MBS are present, surface-induced odd- ν EST correlations are enhanced with vanishing bulk EST correlations. However, bulk and surface contributions of even- ν EST correlations are suppressed. In the trivial regime, at $\nu \rightarrow 0$, both q_e and q_h are purely imaginary in Eqs. (29)-(32), therefore even- ν EST and odd- ν EST correlations show a decay without any oscillation. In the topological regime, at $\nu \rightarrow 0$, both q_e and q_h have both real and imaginary components ($q_h = q_e^*$) in Eqs. (33)-(40), therefore even- ν EST and odd- ν EST correlations exhibit a decay with oscillation inside the superconductor. Even- ν EST correlations are finite both in the presence as well as in the absence of MBS and, thus, do not help in detecting MBS. However, surface odd- ν EST correlations are finite in the presence of MBS, making them a crucial indicator in detecting MBS.

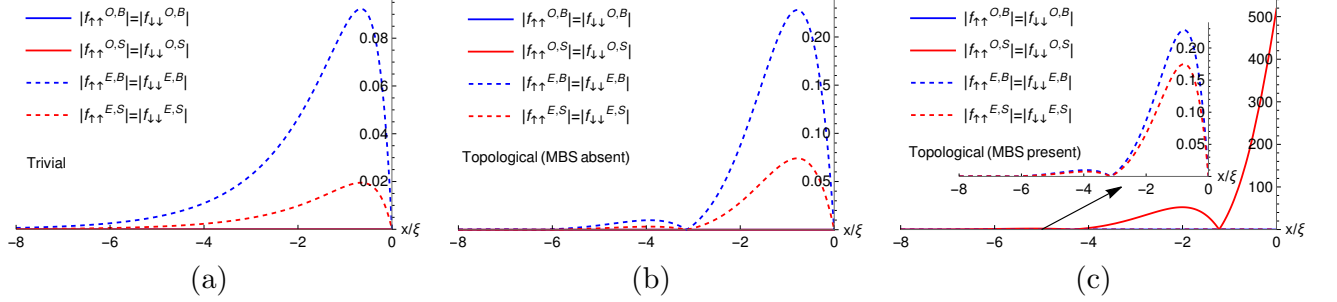


FIG. 3: The absolute values of the bulk and surface contributions to even- ν EST and odd- ν EST correlations within the left superconductor vs. position x for (a) trivial regime, (b) topological regime when MBS is absent ($\varphi = \pi/5$) and, (c) topological regime when MBS is present ($\varphi = \pi$). Parameters: $S = 1/2$, $J = 3$, $\Delta_{p_x} = \sqrt{2}$, $\mu_{p_x} = -1$ (for (a)), $\mu_{p_x} = 1$ (for (b) and (c)), $\bar{x} = 0$, $\varphi = \pi/5$ (for (a) and (b)), $\varphi = \pi$ (for (c)), $\nu \rightarrow 0$.

2. Mixed spin-triplet (MST) superconducting correlations

We now compute the induced even- ν MST and odd- ν MST correlations in our setup. In our work as mentioned before MST correlations are induced in presence of spin flipper. In the **trivial** regime, both the even- ν and odd- ν bulk MST correlations vanish within the left superconductor while both even- ν and odd- ν surface MST components are non-zero, and given by-

$$\text{Bulk even-}\nu \text{ MST: } f_3^{E,B}(x, \bar{x}, \nu) = 0, \quad \text{for } x < 0, \quad (41)$$

$$\begin{aligned} \text{Surface even-}\nu \text{ MST: } f_3^{E,S}(x, \bar{x}, \nu) &= \frac{i\eta}{8(q_h\gamma_e - q_e\gamma_h)} \left(\gamma_h^2 \sqrt{\frac{1 - \gamma_e^2}{1 - \gamma_h^2}} (r_{\uparrow\downarrow}^{e'h'} + r_{\downarrow\uparrow}^{e'h'}) + \gamma_e^2 \sqrt{\frac{1 - \gamma_h^2}{1 - \gamma_e^2}} (r_{\uparrow\downarrow}^{h'e'} + r_{\downarrow\uparrow}^{h'e'}) \right) \\ &\times \left(e^{i(q_h\bar{x} - q_e x)} - e^{i(q_h x - q_e \bar{x})} \right), \quad \text{for } x < 0, \end{aligned} \quad (42)$$

$$\text{Bulk odd-}\nu \text{ MST: } f_3^{O,B}(x, \bar{x}, \nu) = 0, \quad \text{for } x < 0, \quad (43)$$

$$\begin{aligned} \text{Surface odd-}\nu \text{ MST: } f_3^{O,S}(x, \bar{x}, \nu) &= \frac{i\eta}{8(q_h\gamma_e - q_e\gamma_h)} \left(2\gamma_e\gamma_h \left((r_{\uparrow\downarrow}^{e'e'} + r_{\downarrow\uparrow}^{e'e'}) e^{-iq_e(x+\bar{x})} - (r_{\uparrow\downarrow}^{h'h'} + r_{\downarrow\uparrow}^{h'h'}) e^{iq_h(x+\bar{x})} \right) \right. \\ &\left. - \gamma_h^2 \sqrt{\frac{1 - \gamma_e^2}{1 - \gamma_h^2}} (r_{\uparrow\downarrow}^{e'h'} + r_{\downarrow\uparrow}^{e'h'}) + \gamma_e^2 \sqrt{\frac{1 - \gamma_h^2}{1 - \gamma_e^2}} (r_{\uparrow\downarrow}^{h'e'} + r_{\downarrow\uparrow}^{h'e'}) \right) \left(e^{i(q_h\bar{x} - q_e x)} + e^{i(q_h x - q_e \bar{x})} \right), \\ &\text{for } x < 0. \end{aligned} \quad (44)$$

In the **topological** regime, again bulk even- ν MST and odd- ν MST correlations vanish while surface even- ν and odd- ν MST correlations are non-zero within the left superconductor and given as,

$$\text{Bulk even-}\nu \text{ MST: } f_3^{E,B}(x, \bar{x}, \nu) = 0, \text{ for } x < 0, \quad (45)$$

$$\begin{aligned} \text{Surface even-}\nu \text{ MST: } f_3^{E,S}(x, \bar{x}, \nu) &= \frac{i\eta}{8(q_e\gamma_e - q_h\gamma_h)} \left((r_{\uparrow\downarrow}^{e'h'*} + r_{\downarrow\uparrow}^{e'h'*})e^{-i(q_e x - q_h \bar{x})} - (r_{\uparrow\downarrow}^{h'e'*} + r_{\downarrow\uparrow}^{h'e'*})e^{i(q_h x - q_e \bar{x})} \right) \\ &+ \frac{i\eta}{8(q_h\gamma_e - q_e\gamma_h)} \left(-\gamma_h^2 (r_{\uparrow\downarrow}^{e'h'} + r_{\downarrow\uparrow}^{e'h'})e^{-i(q_e \bar{x} - q_h x)} + \gamma_e^2 (r_{\uparrow\downarrow}^{h'e'} + r_{\downarrow\uparrow}^{h'e'})e^{-i(q_e x - q_h \bar{x})} \right), \\ &\text{for } x < 0, \end{aligned} \quad (46)$$

$$\text{Bulk odd-}\nu \text{ MST: } f_3^{O,B}(x, \bar{x}, \nu) = 0, \text{ for } x < 0, \quad (47)$$

$$\begin{aligned} \text{Surface odd-}\nu \text{ MST: } f_3^{O,S}(x, \bar{x}, \nu) &= \frac{i\eta}{8(q_e\gamma_e - q_h\gamma_h)} \left((r_{\uparrow\downarrow}^{e'e'} + r_{\downarrow\uparrow}^{e'e'})e^{-iq_e(x+\bar{x})} - (r_{\uparrow\downarrow}^{h'h'} + r_{\downarrow\uparrow}^{h'h'})e^{iq_h(x+\bar{x})} - (r_{\uparrow\downarrow}^{e'h'*} + r_{\downarrow\uparrow}^{e'h'*}) \right. \\ &\times e^{-i(q_e x - q_h \bar{x})} + (r_{\uparrow\downarrow}^{h'e'*} + r_{\downarrow\uparrow}^{h'e'*})e^{-i(q_e \bar{x} - q_h x)} \left. \right) + \frac{i\eta}{8(q_h\gamma_e - q_e\gamma_h)} \left(\gamma_e\gamma_h (r_{\uparrow\downarrow}^{e'e'} + r_{\downarrow\uparrow}^{e'e'}) \right. \\ &\times e^{-iq_e(x+\bar{x})} - \gamma_e\gamma_h (r_{\uparrow\downarrow}^{h'h'} + r_{\downarrow\uparrow}^{h'h'})e^{iq_h(x+\bar{x})} - \gamma_h^2 (r_{\uparrow\downarrow}^{e'h'} + r_{\downarrow\uparrow}^{e'h'})e^{-i(q_e \bar{x} - q_h x)} \\ &\left. + \gamma_e^2 (r_{\uparrow\downarrow}^{h'e'} + r_{\downarrow\uparrow}^{h'e'})e^{-i(q_e x - q_h \bar{x})} \right), \text{ for } x < 0. \end{aligned} \quad (48)$$

From Eqs. (41)-(48), we see that even- ν MST and odd- ν MST pairings have no bulk contribution and only have surface contribution.

2.1 Zero frequency limit of MST correlations

To understand the behavior of even- ν MST and odd- ν MST correlations when MBS occur, we consider $\nu \rightarrow 0$ limit for both trivial and topological regimes. In the **trivial** regime, at $\nu \rightarrow 0$, $\gamma_e \approx \gamma_h \approx I$, $r_{\uparrow\downarrow}^{e'e'} = r_{\downarrow\uparrow}^{e'e'} = r_{\uparrow\downarrow}^{h'h'} = r_{\downarrow\uparrow}^{h'h'} = 0$, $r_{\uparrow\downarrow}^{e'h'} = r_{\downarrow\uparrow}^{h'e'}$ and, $r_{\uparrow\downarrow}^{e'h'} = r_{\downarrow\uparrow}^{h'e'}$. We note that the Andreev reflection amplitudes are purely real. Thus from Eqs. (41)-(44) we get,

$$\text{Bulk even-}\nu \text{ MST: } f_3^{E,B}(x, \bar{x}, \nu \rightarrow 0) = 0 \text{ for } x < 0, \quad (49)$$

$$\text{Surface even-}\nu \text{ MST: } f_3^{E,S}(x, \bar{x}, \nu \rightarrow 0) = \frac{\eta}{4(q_h - q_e)} \left((r_{\uparrow\downarrow}^{e'h'} + r_{\downarrow\uparrow}^{e'h'}) (e^{-i(q_e \bar{x} - q_h x)} - e^{-i(q_e x - q_h \bar{x})}) \right), \text{ for } x < 0, \quad (50)$$

$$\text{Bulk odd-}\nu \text{ MST: } f_3^{O,B}(x, \bar{x}, \nu \rightarrow 0) = 0, \text{ for } x < 0, \quad (51)$$

$$\text{Surface odd-}\nu \text{ MST: } f_3^{O,S}(x, \bar{x}, \nu \rightarrow 0) = 0 \text{ for } x < 0. \quad (52)$$

Bulk MST correlations vanish for both even- ν and odd- ν , and surface MST correlations are non-zero for even- ν while for odd- ν , they too disappear. In the **topological** regime, at $\nu \rightarrow 0$, $\gamma_h \approx -\gamma_e$, $(q_e\gamma_e - q_h\gamma_h)\gamma_e^2 + (q_h\gamma_e - q_e\gamma_h) \ll 1$, $r_{\uparrow\downarrow}^{e'e'} = r_{\uparrow\downarrow}^{h'h'*}$, $r_{\downarrow\uparrow}^{e'e'} = r_{\downarrow\uparrow}^{h'h'*}$ and when MBS are **absent** ($\varphi \neq \pi$), normal and Andreev reflection amplitudes $r_{\uparrow\downarrow}^{e'h'} = r_{\downarrow\uparrow}^{h'e'} = r_{\uparrow\downarrow}^{h'h'} = r_{\downarrow\uparrow}^{e'h'} = r_{\uparrow\downarrow}^{e'h'} = r_{\downarrow\uparrow}^{h'e'} = 0$, thus from Eqs. (45)-(48) we obtain,

$$\text{Bulk even-}\nu \text{ MST: } f_3^{E,B}(x, \bar{x}, \nu \rightarrow 0) = 0, \text{ for } x < 0, \quad (53)$$

$$\text{Surface even-}\nu \text{ MST: } f_3^{E,S}(x, \bar{x}, \nu \rightarrow 0) = 0, \text{ for } x < 0, \quad (54)$$

$$\text{Bulk odd-}\nu \text{ MST: } f_3^{O,B}(x, \bar{x}, \nu \rightarrow 0) = 0, \text{ for } x < 0, \quad (55)$$

$$\text{Surface odd-}\nu \text{ MST: } f_3^{O,S}(x, \bar{x}, \nu \rightarrow 0) = 0, \text{ for } x < 0. \quad (56)$$

All correlations, both bulk and surface, for either odd- ν or even- ν vanish. Finally, in the **topological** regime, at $\nu \rightarrow 0$, when MBS are **present** ($\varphi = \pi$), normal reflection amplitudes satisfy $r_{\uparrow\downarrow}^{e'e'} = r_{\uparrow\downarrow}^{h'h'*}$, $r_{\downarrow\uparrow}^{e'e'} = r_{\downarrow\uparrow}^{h'h'*}$ and, Andreev reflection amplitudes satisfy $r_{\uparrow\downarrow}^{e'h'} = r_{\uparrow\downarrow}^{h'e'*}$, $r_{\downarrow\uparrow}^{e'h'} = r_{\downarrow\uparrow}^{h'e'*}$ with $\text{Im}[r_{\uparrow\downarrow}^{e'h'}] \gg 1$, $\text{Im}[r_{\downarrow\uparrow}^{e'h'}] \gg 1$, thus from Eqs. (45)-(48) we see surface MST correlations are finite for both even- ν and odd- ν while bulk MST correlations

vanish for both even- ν and odd- ν .

$$\text{Bulk even-}\nu \text{ MST: } f_3^{E,B}(x, \bar{x}, \nu \rightarrow 0) = 0, \text{ for } x < 0, \quad (57)$$

$$\begin{aligned} \text{Surface even-}\nu \text{ MST: } f_3^{E,S}(x, \bar{x}, \nu \rightarrow 0) &= \frac{i\eta}{8\gamma_e(q_e + q_h)} \left((r_{\uparrow\downarrow}^{h'e'} + r_{\downarrow\uparrow}^{h'e'}) (1 + \gamma_e^2) e^{-i(q_e x - q_h \bar{x})} - (r_{\uparrow\downarrow}^{e'h'} + r_{\downarrow\uparrow}^{e'h'}) (1 + \gamma_h^2) \right. \\ &\quad \left. \times e^{i(q_h x - q_e \bar{x})} \right), \text{ for } x < 0, \end{aligned} \quad (58)$$

$$\text{Bulk odd-}\nu \text{ MST: } f_3^{O,B}(x, \bar{x}, \nu \rightarrow 0) = 0, \text{ for } x < 0, \quad (59)$$

$$\begin{aligned} \text{Surface odd-}\nu \text{ MST: } f_3^{O,S}(x, \bar{x}, \nu \rightarrow 0) &= \frac{i\eta}{8\gamma_e(q_e + q_h)} \left(2(r_{\uparrow\downarrow}^{e'e'} + r_{\downarrow\uparrow}^{e'e'}) e^{-iq_e(x+\bar{x})} - 2(r_{\uparrow\downarrow}^{h'h'} + r_{\downarrow\uparrow}^{h'h'}) e^{iq_h(x+\bar{x})} - (r_{\uparrow\downarrow}^{h'e'} \right. \\ &\quad \left. + r_{\downarrow\uparrow}^{h'e'}) (1 - \gamma_e^2) e^{-i(q_e x - q_h \bar{x})} + (r_{\uparrow\downarrow}^{e'h'} + r_{\downarrow\uparrow}^{e'h'}) (1 - \gamma_h^2) e^{i(q_h x - q_e \bar{x})} \right), \text{ for } x < 0. \end{aligned} \quad (60)$$

Surface and bulk components of even- ν MST and odd- ν MST correlations, at $\nu \rightarrow 0$ in the superconducting region, are plotted as function of position x in Fig. 4. Similar to Fig. 3, we consider three cases: (a) trivial regime, (b) topological regime when MBS are absent, and (c) topological regime when MBS are present. From Fig. 4(a), we see that, in the trivial regime, surface even- ν MST correlations are finite and show a decay without any oscillation, but odd- ν MST correlations vanish. In Fig. 4(b), in the topological regimes when MBS are absent ($\varphi = \pi/5$), both even- ν MST and odd- ν MST correlations are zero. Finally, in Fig. 4(c), we see that when MBS are present, surface odd- ν MST correlations are finite with very large magnitude while surface even- ν MST correlations are very small. Further, surface even- ν MST correlations are finite in the trivial regime when MBS are absent, as well as in the topological regime when MBS are present and, thus, do not distinguish MBS. Surface Odd- ν MST correlations are finite in the topological regime when MBS are present, but vanish in the absence of MBS. **Therefore, induced surface odd- ν MST correlations imply presence of MBS. This is the main result of our work.**

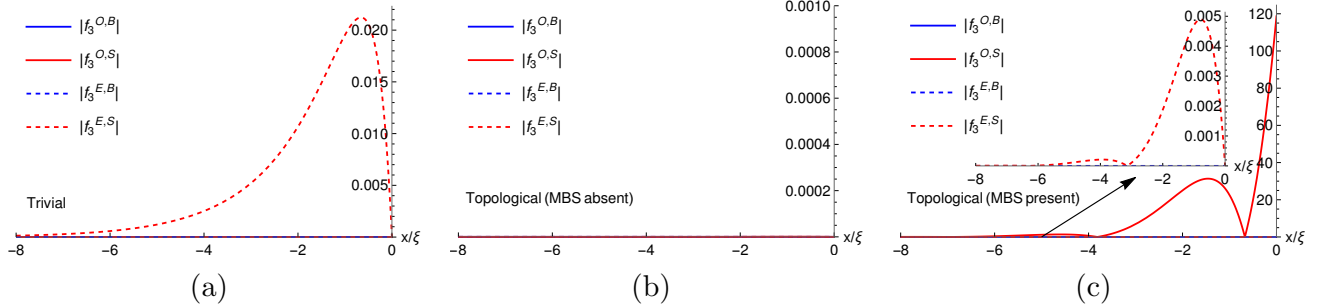


FIG. 4: The absolute values of the bulk and surface contributions to even- ν MST and odd- ν MST correlations within the left superconductor vs. position x for (a) trivial regime, (b) topological regime when MBS is absent ($\varphi = \pi/5$) and, (c) topological regime when MBS is present ($\varphi = \pi$). Parameters: $S = 1/2$, $J = 3$, $\Delta_{p_x} = \sqrt{2}$, $\mu_{p_x} = -1$ (for (a)), $\mu_{p_x} = 1$ (for (b) and (c)), $\bar{x} = 0$, $\varphi = \pi/5$ (for (a) and (b)), $\varphi = \pi$ (for (c)), $\nu \rightarrow 0$.

IV. ANALYSIS

We compare our results in Table I both when SF is present and when it is absent. Even- ν SS and odd- ν SS correlations always vanish in both the trivial and topological regimes irrespective of spin flip scattering and therefore we do not put them in Table I. We notice that only even- ν EST correlations are finite in bulk in presence as well as in absence of MBS irrespective of spin flip scattering. Thus, bulk component of EST correlations do not contribute to the identification of MBS. Surface contributions of even- ν EST correlations are finite both in trivial and topological regimes in presence of spin flip scattering. Surface components of even- ν MST correlations are finite in the topological regimes when MBS are present and also in the trivial regimes in presence of spin flip scattering. Thus, even- ν EST and even- ν MST correlations can not help in detecting MBS. Surface contributions of odd- ν EST correlations are nonzero in the presence of MBS; however, they vanish when MBS are absent regardless of spin flip scattering. Surface components of odd- ν MST correlations are present when MBS occur, but they are absent when MBS are absent in presence of spin flip scattering. Thus, surface-induced odd- ν EST and odd- ν MST correlations can distinguish MBS

in the presence of spin flip scattering. In our work, when SF is absent, surface odd- ν MST correlations will also be absent. Thus, spin flip scattering helps in detecting MBS via inducing surface odd- ν MST correlation in the presence of MBS.

TABLE I: Comparing odd- and even- ν correlations at $\nu \rightarrow 0$ in presence and absence of SF

		Topological (MBS present)		Topological (MBS absent)		Trivial	
		SF present	SF absent	SF present	SF absent	SF present	SF absent
Odd- ν EST	Bulk	Absent	Absent	Absent	Absent	Absent	Absent
	Surface	Present	Present	Absent	Absent	Absent	Absent
Even- ν EST	Bulk	Present	Present	Present	Present	Present	Present
	Surface	Present	Present	Present	Present	Present	Absent
Odd- ν MST	Bulk	Absent	Absent	Absent	Absent	Absent	Absent
	Surface	Present	Absent	Absent	Absent	Absent	Absent
Even- ν MST	Bulk	Absent	Absent	Absent	Absent	Absent	Absent
	Surface	Present	Absent	Absent	Absent	Present	Absent

Next, in Table II we explain the reasons behind our results. In the trivial regime, for $\nu \rightarrow 0$, and for MBS absent, normal reflection amplitudes without spin-flip are zero, i.e., $r_{\uparrow\uparrow}^{e'e'} = r_{\downarrow\downarrow}^{e'e'} = r_{\uparrow\uparrow}^{h'h'} = r_{\downarrow\downarrow}^{h'h'} = 0$ while Andreev reflection amplitudes without spin-flip satisfy $r_{\uparrow\uparrow}^{e'h'} = r_{\uparrow\uparrow}^{h'e'} \neq 0$, $r_{\downarrow\downarrow}^{e'h'} = r_{\downarrow\downarrow}^{h'e'} \neq 0$ which lead to finite surface even- ν EST correlations with vanishing surface odd- ν EST correlations, see Eqs. (30), (32). Further, in the trivial regime, normal reflection amplitudes with spin-flip are zero, i.e., $r_{\uparrow\downarrow}^{e'e'} = r_{\downarrow\uparrow}^{e'e'} = r_{\uparrow\downarrow}^{h'h'} = r_{\downarrow\uparrow}^{h'h'} = 0$ while Andreev reflection amplitudes with spin-flip satisfy $r_{\uparrow\downarrow}^{e'h'} = r_{\uparrow\downarrow}^{h'e'} \neq 0$, $r_{\downarrow\uparrow}^{e'h'} = r_{\downarrow\uparrow}^{h'e'} \neq 0$ which lead to finite surface even- ν MST correlations and vanishing surface odd- ν MST correlations, as evident from Eqs. (50), (52).

In the topological regime for $\nu \rightarrow 0$ and when MBS are absent ($\varphi \neq \pi$), normal reflection amplitudes without spin-flip satisfy $r_{\uparrow\uparrow}^{e'e'} = r_{\downarrow\downarrow}^{e'e'} = r_{\uparrow\uparrow}^{h'h'} = r_{\downarrow\downarrow}^{h'h'} = 0$ while Andreev reflection amplitudes without spin-flip are equal, i.e., $r_{\uparrow\downarrow}^{e'h'} = r_{\downarrow\uparrow}^{e'h'} = r_{\uparrow\downarrow}^{h'e'} = r_{\downarrow\uparrow}^{h'e'} \neq 0$ which lead to finite surface even- ν EST correlations and vanishing surface odd- ν EST correlations, see Eqs. (34), (36). In the topological regime, when MBS are absent, normal reflection amplitudes with spin-flip satisfy $r_{\uparrow\downarrow}^{e'e'} = r_{\downarrow\uparrow}^{e'e'} = r_{\uparrow\downarrow}^{h'h'} = r_{\downarrow\uparrow}^{h'h'} = 0$ while spin flip Andreev reflection amplitudes are again vanishing, i.e., $r_{\uparrow\downarrow}^{e'h'} = r_{\downarrow\uparrow}^{e'h'} = r_{\uparrow\downarrow}^{h'e'} = r_{\downarrow\uparrow}^{h'e'} = 0$ which lead to vanishing surface even- ν MST and surface odd- ν MST correlations, as evident from Eqs. (54), (56).

Finally, in the topological regime for $\nu \rightarrow 0$ and when MBS are present ($\varphi = \pi$), normal reflection amplitudes without spin-flip satisfy $r_{\uparrow\uparrow}^{e'e'} = r_{\uparrow\uparrow}^{h'h'*}$, $r_{\downarrow\downarrow}^{e'e'} = r_{\downarrow\downarrow}^{h'h'*}$ while Andreev reflection amplitudes without spin-flip satisfy $r_{\uparrow\uparrow}^{e'h'} = r_{\uparrow\uparrow}^{h'e'*}$, $r_{\downarrow\downarrow}^{e'h'} = r_{\downarrow\downarrow}^{h'e'*}$ which lead to finite surface even- ν EST and surface odd- ν EST correlations, see Eqs. (38), (40). In this regime, normal reflection amplitudes with spin-flip satisfy $r_{\uparrow\downarrow}^{e'e'} = r_{\uparrow\downarrow}^{h'h'*}$, $r_{\downarrow\uparrow}^{e'e'} = r_{\downarrow\uparrow}^{h'h'*}$ while Andreev reflection amplitudes with spin-flip satisfy $r_{\uparrow\downarrow}^{e'h'} = r_{\uparrow\downarrow}^{h'e'*}$, $r_{\downarrow\uparrow}^{e'h'} = r_{\downarrow\uparrow}^{h'e'*}$ which lead to finite surface even- ν MST and finite surface odd- ν MST correlations, as evident from Eqs. (58), (60). It is important to note that both normal and Andreev reflection amplitudes follow distinct conditions in the presence and absence of MBS. These differing conditions lead to distinguishable results under these two scenarios.

TABLE II: Normal and Andreev reflection amplitudes at $\nu \rightarrow 0$ in trivial and topological regimes (MBS absent and MBS present)

	Normal reflection amplitudes without spin-flip	Normal reflection amplitudes with spin-flip	Andreev reflection amplitudes without spin-flip	Andreev reflection amplitudes with spin-flip
Trivial	$r_{\uparrow\uparrow}^{e'e'} = r_{\downarrow\downarrow}^{e'e'} = r_{\uparrow\uparrow}^{h'h'} = r_{\downarrow\downarrow}^{h'h'} = 0$, i.e., they are vanishing	$r_{\uparrow\downarrow}^{e'e'} = r_{\downarrow\uparrow}^{e'e'} = r_{\uparrow\downarrow}^{h'h'} = r_{\downarrow\uparrow}^{h'h'} = 0$, i.e., they are vanishing	$r_{\uparrow\uparrow}^{e'h'} = r_{\uparrow\uparrow}^{h'e'}$, $r_{\downarrow\downarrow}^{e'h'} = r_{\downarrow\downarrow}^{h'e'}$, they are finite (real)	$r_{\uparrow\downarrow}^{e'h'} = r_{\uparrow\downarrow}^{h'e'}$, $r_{\downarrow\uparrow}^{e'h'} = r_{\downarrow\uparrow}^{h'e'}$, they are finite (real)
Topological (MBS absent)	$r_{\uparrow\uparrow}^{e'e'} = r_{\downarrow\downarrow}^{e'e'} = r_{\uparrow\uparrow}^{h'h'} = r_{\downarrow\downarrow}^{h'h'} = 0$, i.e., they are vanishing	$r_{\uparrow\downarrow}^{e'e'} = r_{\downarrow\uparrow}^{e'e'} = r_{\uparrow\downarrow}^{h'h'} = r_{\downarrow\uparrow}^{h'h'} = 0$, i.e., they are vanishing	$r_{\uparrow\uparrow}^{e'h'} = r_{\downarrow\downarrow}^{e'h'} = r_{\uparrow\uparrow}^{h'e'} = r_{\downarrow\downarrow}^{h'e'}$, they are finite (imaginary)	$r_{\uparrow\downarrow}^{e'h'} = r_{\downarrow\uparrow}^{e'h'} = r_{\uparrow\downarrow}^{h'e'} = r_{\downarrow\uparrow}^{h'e'}$, they are vanishing
Topological (MBS present)	$r_{\uparrow\uparrow}^{e'e'} = r_{\uparrow\uparrow}^{h'h'*}$, $r_{\downarrow\downarrow}^{e'e'} = r_{\downarrow\downarrow}^{h'h'*}$, they are finite (complex)	$r_{\uparrow\downarrow}^{e'e'} = r_{\uparrow\downarrow}^{h'h'*}$, $r_{\downarrow\uparrow}^{e'e'} = r_{\downarrow\uparrow}^{h'h'*}$, they are finite (complex)	$r_{\uparrow\uparrow}^{e'h'} = r_{\uparrow\uparrow}^{h'e'*}$, $r_{\downarrow\downarrow}^{e'h'} = r_{\downarrow\downarrow}^{h'e'*}$, they are finite (complex)	$r_{\uparrow\downarrow}^{e'h'} = r_{\uparrow\downarrow}^{h'e'*}$, $r_{\downarrow\uparrow}^{e'h'} = r_{\downarrow\uparrow}^{h'e'*}$, they are finite (complex)

In Ref. [41], it is found that within the topological phase, the spatial variation of the odd- ν EST pairing amplitude

coincides with that of the local density of states at zero energy in a semi-infinite Kitaev chain. This suggests a direct link between the wave function of Majorana fermions and the odd- ν EST pairing amplitude at low frequencies. Further, in Ref. [42], the authors propose that the interaction between Majorana zero modes and a spin-polarized nanowire leads to the emergence of odd- ν EST pairing in the nanowire. In addition, in Ref. [43], the authors examine the stability of odd- ν EST pairing induced in a nanowire coupled with Majorana zero modes, particularly when the coupling between them exhibits complexity. Nevertheless, in Refs. [41]-[43], odd- ν MST pairing does not emerge, and they do not offer any methodology for MBS detection through odd- ν pairing. This distinction sets our work apart from theirs.

V. EXPERIMENTAL IMPLEMENTATION AND SUMMARY

Our system as depicted in Fig. 1 can be implemented in a laboratory setting. p_x -wave pairing is experimentally found in the quasi 1D organic superconductors (TMTSF)₂PF₆[57, 58]. Replacing the spin flipper at the p_x - p_x superconductor interface must be technically feasible. From an experimental perspective, magnetic molecules such as the Mn₄O₃ complex, featuring a spin quantum number of $S = 9/2$ [59], offer a partial analog for the spin flipper. It is worth noting that the interior dynamics of such a high-spin molecule may exhibit notable distinctions from those of our spin flipper. Nonetheless, the spin flipper can effectively emulate half-integer spin states, along with capturing the related spin magnetic moment of the molecule. This enables a substantial approximation of electron interactions with such entities.

In summary, our investigation reveals that surface odd- ν ST correlations provide a distinct signature of the presence of MBS in p_x superconductor-SF- p_x superconductor Josephson junction. Surface even- ν ST correlations, on the other hand, remain finite irrespective of the existence of MBS, rendering them unsuitable for MBS detection. In contrast, surface odd- ν ST correlations exhibit finite values exclusively in the presence of MBS, and they vanish in the absence of MBS. Spin flip scattering plays a crucial role in detecting MBS via inducing surface odd- ν MST correlations in their presence. While the relationship between MBS and odd- ν pairing is explored in Refs. [39]-[43], odd- ν MST correlations do not emerge, and they do not offer a method to detect MBS through odd- ν pairing. This sets our work apart from them. Thus, our findings underscore the utility of surface odd- ν ST correlations as an effective tool for discerning the presence of MBS.

ACKNOWLEDGMENTS

This research received funding from the following grants: 1. SERB Grant No. CRG/2019/006258 for the study of Josephson junctions with strained Dirac materials and their applications in quantum information processing, and 2. SERB MATRICS Grant No. MTR/2018/000070 for investigating Nash equilibrium versus Pareto optimality in N-Player games.

Appendix A: Analytical formulas for Anomalous Green's functions

In this section, analytical formulas for Anomalous Green's functions (\mathcal{G}_{eh}^r) are provided. We calculate EST and MST correlations using \mathcal{G}_{eh}^r . Retarded Green's functions \mathcal{G}^r are derived by substituting the wavefunctions from Eq. (3)

into Eq. (12), with r_{ij}^{nn} determined using Eq. (7). In the trivial regime for \mathcal{G}_{eh}^r we get,

$$\begin{aligned}
[\mathcal{G}_{eh}^r]_{\uparrow\uparrow} &= \frac{i\eta}{2(q_h\gamma_e - q_e\gamma_h)} \left(-\gamma_e\gamma_h e^{iq_e|x-\bar{x}|} \text{sgn}(x-\bar{x}) + \gamma_e\gamma_h e^{-iq_h|x-\bar{x}|} + r_{\uparrow\uparrow}^{e'e'} \gamma_e\gamma_h e^{-iq_e(x+\bar{x})} - r_{\uparrow\uparrow}^{h'h'} \gamma_e\gamma_h e^{iq_h(x+\bar{x})} \right. \\
&\quad \left. - r_{\uparrow\uparrow}^{e'h'} \gamma_h^2 \sqrt{\frac{1-\gamma_e^2}{1-\gamma_h^2}} e^{i(q_hx-q_e\bar{x})} + r_{\uparrow\uparrow}^{h'e'} \gamma_e^2 \sqrt{\frac{1-\gamma_h^2}{1-\gamma_e^2}} e^{-i(q_ex-q_h\bar{x})} \right), \\
[\mathcal{G}_{eh}^r]_{\downarrow\downarrow} &= \frac{i\eta}{2(q_h\gamma_e - q_e\gamma_h)} \left(-\gamma_e\gamma_h e^{iq_e|x-\bar{x}|} \text{sgn}(x-\bar{x}) + \gamma_e\gamma_h e^{-iq_h|x-\bar{x}|} + r_{\downarrow\downarrow}^{e'e'} \gamma_e\gamma_h e^{-iq_e(x+\bar{x})} - r_{\downarrow\downarrow}^{h'h'} \gamma_e\gamma_h e^{iq_h(x+\bar{x})} \right. \\
&\quad \left. - r_{\downarrow\downarrow}^{e'h'} \gamma_h^2 \sqrt{\frac{1-\gamma_e^2}{1-\gamma_h^2}} e^{i(q_hx-q_e\bar{x})} + r_{\downarrow\downarrow}^{h'e'} \gamma_e^2 \sqrt{\frac{1-\gamma_h^2}{1-\gamma_e^2}} e^{-i(q_ex-q_h\bar{x})} \right), \\
[\mathcal{G}_{eh}^r]_{\uparrow\downarrow} &= \frac{i\eta}{2(q_h\gamma_e - q_e\gamma_h)} \left(r_{\downarrow\uparrow}^{e'e'} \gamma_e\gamma_h e^{-iq_e(x+\bar{x})} - r_{\downarrow\uparrow}^{h'h'} \gamma_e\gamma_h e^{iq_h(x+\bar{x})} - r_{\downarrow\uparrow}^{e'h'} \gamma_h^2 \sqrt{\frac{1-\gamma_e^2}{1-\gamma_h^2}} e^{i(q_hx-q_e\bar{x})} + r_{\downarrow\uparrow}^{h'e'} \gamma_e^2 \sqrt{\frac{1-\gamma_h^2}{1-\gamma_e^2}} \right. \\
&\quad \left. e^{-i(q_ex-q_h\bar{x})} \right), \\
[\mathcal{G}_{eh}^r]_{\downarrow\uparrow} &= \frac{i\eta}{2(q_h\gamma_e - q_e\gamma_h)} \left(r_{\uparrow\downarrow}^{e'e'} \gamma_e\gamma_h e^{-iq_e(x+\bar{x})} - r_{\uparrow\downarrow}^{h'h'} \gamma_e\gamma_h e^{iq_h(x+\bar{x})} - r_{\uparrow\downarrow}^{e'h'} \gamma_h^2 \sqrt{\frac{1-\gamma_e^2}{1-\gamma_h^2}} e^{i(q_hx-q_e\bar{x})} + r_{\uparrow\downarrow}^{h'e'} \gamma_e^2 \sqrt{\frac{1-\gamma_h^2}{1-\gamma_e^2}} \right. \\
&\quad \left. e^{-i(q_ex-q_h\bar{x})} \right).
\end{aligned} \tag{61}$$

In the topological regime for \mathcal{G}_{eh}^r we get,

$$\begin{aligned}
[\mathcal{G}_{eh}^r]_{\uparrow\uparrow} &= \frac{i\eta}{2(q_h\gamma_e - q_e\gamma_h)} \left(-\gamma_e\gamma_h e^{iq_e|x-\bar{x}|} \text{sgn}(x-\bar{x}) + \gamma_e\gamma_h e^{-iq_h|x-\bar{x}|} + r_{\uparrow\uparrow}^{e'e'} \gamma_e\gamma_h e^{-iq_e(x+\bar{x})} - r_{\uparrow\uparrow}^{h'h'} e^{iq_h(x+\bar{x})} - r_{\uparrow\uparrow}^{e'h'} \gamma_h^2 \right. \\
&\quad \left. e^{i(q_hx-q_e\bar{x})} + r_{\uparrow\uparrow}^{h'e'} \gamma_e^2 e^{-i(q_ex-q_h\bar{x})} \right), \\
[\mathcal{G}_{eh}^r]_{\downarrow\downarrow} &= \frac{i\eta}{2(q_h\gamma_e - q_e\gamma_h)} \left(-\gamma_e\gamma_h e^{iq_e|x-\bar{x}|} \text{sgn}(x-\bar{x}) + \gamma_e\gamma_h e^{-iq_h|x-\bar{x}|} + r_{\downarrow\downarrow}^{e'e'} \gamma_e\gamma_h e^{-iq_e(x+\bar{x})} - r_{\downarrow\downarrow}^{h'h'} e^{iq_h(x+\bar{x})} - r_{\downarrow\downarrow}^{e'h'} \gamma_h^2 \right. \\
&\quad \left. e^{i(q_hx-q_e\bar{x})} + r_{\downarrow\downarrow}^{h'e'} \gamma_e^2 e^{-i(q_ex-q_h\bar{x})} \right), \\
[\mathcal{G}_{eh}^r]_{\uparrow\downarrow} &= \frac{i\eta}{2(q_h\gamma_e - q_e\gamma_h)} \left(r_{\downarrow\uparrow}^{e'e'} \gamma_e\gamma_h e^{-iq_e(x+\bar{x})} - r_{\downarrow\uparrow}^{h'h'} \gamma_e\gamma_h e^{iq_h(x+\bar{x})} - r_{\downarrow\uparrow}^{e'h'} \gamma_h^2 e^{i(q_hx-q_e\bar{x})} + r_{\downarrow\uparrow}^{h'e'} \gamma_e^2 e^{-i(q_ex-q_h\bar{x})} \right), \\
[\mathcal{G}_{eh}^r]_{\downarrow\uparrow} &= \frac{i\eta}{2(q_h\gamma_e - q_e\gamma_h)} \left(r_{\uparrow\downarrow}^{e'e'} \gamma_e\gamma_h e^{-iq_e(x+\bar{x})} - r_{\uparrow\downarrow}^{h'h'} \gamma_e\gamma_h e^{iq_h(x+\bar{x})} - r_{\uparrow\downarrow}^{e'h'} \gamma_h^2 e^{i(q_hx-q_e\bar{x})} + r_{\uparrow\downarrow}^{h'e'} \gamma_e^2 e^{-i(q_ex-q_h\bar{x})} \right).
\end{aligned} \tag{62}$$

-
- [1] J. Bardeen, L. N. Cooper, and J. R. Schrieffer, Theory of Superconductivity, Phys. Rev. 108, 1175 (1957).
[2] M. Sigrist and K. Ueda, Phenomenological theory of unconventional superconductivity, Rev. Mod. Phys. 63, 239 (1991).
[3] J. Linder and A. V. Balatsky, Odd-frequency superconductivity, Rev. Mod. Phys. 91, 045005 (2019).
[4] Y. Tanaka, M. Sato, and N. Nagaosa, Symmetry and topology in superconductors -odd-frequency pairing and edge states-, J. Phys. Soc. Jpn. 81, 011013 (2012).
[5] J. Cayao, C. Triola, and A. M. Black-Schaffer, Odd-frequency superconducting pairing in one-dimensional systems, Eur. Phys. J.: Spec. Top. 229, 545 (2020).
[6] V. L. Berezinskii, New model of the anisotropic phase of superfluid ^3He , Zh. Eksp. Teor. Fiz. 20, 628 (1974) [JETP Lett. 20, 287 (1974)].
[7] F. S. Bergeret, A. F. Volkov, and K. B. Efetov, Long-Range Proximity Effects in Superconductor-Ferromagnet Structures, Phys. Rev. Lett. 86, 4096 (2001).
[8] F. S. Bergeret, A. F. Volkov, and K. B. Efetov, Manifestation of triplet superconductivity in superconductor-ferromagnet structures, Phys. Rev. B 68, 064513 (2003).
[9] A. Balatsky and E. Abrahams, New class of singlet superconductors which break the time reversal and parity, Phys. Rev. B 45, 13125 (1992).
[10] E. Abrahams, A. Balatsky, D. J. Scalapino, and J. R. Schrieffer, Properties of odd-gap superconductors, Phys. Rev. B 52, 1271 (1995).

- [11] Y. Tanaka, Y. Tanuma, and A. A. Golubov, Odd-frequency pairing in normal-metal/superconductor junctions, *Phys. Rev. B* 76, 054522 (2007).
- [12] F. S. Bergeret, A. F. Volkov, and K. B. Efetov, Long-Range Proximity Effects in Superconductor-Ferromagnet Structures, *Phys. Rev. Lett.* 86, 4096 (2001).
- [13] Y. Tanaka, A. A. Golubov, S. Kashiwaya, and M. Ueda, Anomalous Josephson Effect between Even- and Odd-Frequency Superconductors, *Phys. Rev. Lett.* 99, 037005 (2007).
- [14] T. Yokoyama, Y. Tanaka, and A. A. Golubov, Manifestation of the odd-frequency spin-triplet pairing state in diffusive ferromagnet/superconductor junctions, *Phys. Rev. B* 75, 134510 (2007).
- [15] A. M. Black-Schaffer and A. V. Balatsky, Proximity-induced unconventional superconductivity in topological insulators, *Phys. Rev. B* 87, 220506(R) (2013).
- [16] J. Linder, A. Sudbø, T. Yokoyama, R. Grein, and M. Eschrig, Signature of odd-frequency pairing correlations induced by a magnetic interface, *Phys. Rev. B* 81, 214504 (2010).
- [17] J. Linder, T. Yokoyama, A. Sudbø, and M. Eschrig, Pairing Symmetry Conversion by Spin-Active Interfaces in Magnetic Normal-Metal-Superconductor Junctions, *Phys. Rev. Lett.* 102, 107008 (2009).
- [18] S. Pal and C. Benjamin, Exciting odd-frequency equal spin-triplet correlations at metal-superconductor interfaces, *Phys. Rev. B* 104, 054519 (2021).
- [19] A. F. Volkov, A. Anishchanka, and K. B. Efetov, Odd triplet superconductivity in a superconductor/ferromagnet system with a spiral magnetic structure, *Phys. Rev. B* 73, 104412 (2006).
- [20] F. S. Bergeret, A. F. Volkov, and K. B. Efetov, Odd triplet superconductivity and related phenomena in superconductor-ferromagnet structures, *Rev. Mod. Phys.* 77, 1321 (2005).
- [21] M. Eschrig, J. Kopu, J. C. Cuevas, and Gerd Schön, Theory of Half-Metal/Superconductor Heterostructures, *Phys. Rev. Lett.* 90, 137003 (2003).
- [22] A. M. Black-Schaffer and A. V. Balatsky, Odd-frequency superconducting pairing in topological insulators, *Phys. Rev. B* 86, 144506 (2012).
- [23] F. Crépin, P. Buset, and B. Trauzettel, Odd-frequency triplet superconductivity at the helical edge of a topological insulator, *Phys. Rev. B* 92, 100507(R) (2015).
- [24] P. Buset, B. Lu, G. Tkachov, Y. Tanaka, E. M. Hankiewicz, and B. Trauzettel, Superconducting proximity effect in three-dimensional topological insulators in the presence of a magnetic field, *Phys. Rev. B* 92, 205424 (2015).
- [25] M. Eschrig, T. Löfwander, T. Champel, J. C. Cuevas, J. Kopu, and G. Schön, Symmetries of Pairing Correlations in Superconductor-Ferromagnet Nanostructures, *J. Low Temp. Phys.* 147, 457 (2007).
- [26] A. F. Volkov, F. S. Bergeret, and K. B. Efetov, Odd Triplet Superconductivity in Superconductor-Ferromagnet Multilayered Structures, *Phys. Rev. Lett.* 90, 117006 (2003).
- [27] Y. V. Fominov, A. F. Volkov, and K. B. Efetov, Josephson effect due to the long-range odd-frequency triplet superconductivity in SFS junctions with Néel domain walls, *Phys. Rev. B* 75, 104509 (2007).
- [28] A. I. Buzdin, Proximity effects in superconductor-ferromagnet heterostructures, *Rev. Mod. Phys.* 77, 935 (2005).
- [29] S.-Y. Hwang, P. Buset, and B. Sothmann, Odd-frequency superconductivity revealed by thermopower, *Phys. Rev. B* 98, 161408(R) (2018).
- [30] S. Tamura, Y. Tanaka, and T. Yokoyama, Generation of polarized spin-triplet Cooper pairings by magnetic barriers in superconducting junctions, *Phys. Rev. B* 107, 054501 (2023).
- [31] C. Triola and A. V. Balatsky, Pair symmetry conversion in driven multiband superconductors, *Phys. Rev. B* 95, 224518 (2017).
- [32] C. Triola and A. V. Balatsky, Odd-frequency superconductivity in driven systems, *Phys. Rev. B* 94, 094518 (2016).
- [33] J. Linder and J. W. A. Robinson, Superconducting spintronics, *Nat. Phys.* 11, 307-315 (2015).
- [34] A. Y. Kitaev, Unpaired Majorana fermions in quantum wires, *Phys. Usp.* 44, 131 (2001).
- [35] C. Nayak, S. H. Simon, A. Stern, M. Freedman, and S. Das Sarma, Non-Abelian anyons and topological quantum computation, *Rev. Mod. Phys.* 80, 1083 (2008).
- [36] S. D. Sarma, M. Freedman, and C. Nayak, Majorana zero modes and topological quantum computation, *npj Quantum Inform.* 1, 15001 (2015).
- [37] C. Schrade and L. Fu, Majorana Superconducting Qubit, *Phys. Rev. Lett.* 121, 267002 (2018).
- [38] H.-J. Kwon, K. Sengupta, and V. M. Yakovenko, Fractional ac Josephson effect in p - and d -wave superconductors, *Eur. Phys. J. B* 37, 349 (2004).
- [39] A. Tsintzis, A. M. Black-Schaffer, and J. Cayao, Odd-frequency superconducting pairing in Kitaev-based junctions, *Phys. Rev. B* 100, 115433 (2019).
- [40] Y. Asano and Y. Tanaka, Majorana fermions and odd-frequency Cooper pairs in a normal-metal nanowire proximity-coupled to a topological superconductor, *Phys. Rev. B* 87, 104513 (2013).
- [41] D. Takagi, S. Tamura, Y. Tanaka, Odd-frequency pairing and proximity effect in Kitaev chain systems including topological critical point, *Phys. Rev. B* 101, 024509 (2020).
- [42] S.-P. Lee, R. M. Lutchyn, and J. Maciejko, Odd-frequency superconductivity in a nanowire coupled to Majorana zero modes, *Phys. Rev. B* 95, 184506 (2017).
- [43] D. Kuzmanovski, A. M. Black-Schaffer, and J. Cayao, Suppression of odd-frequency pairing by phase disorder in a nanowire coupled to Majorana zero modes, *Phys. Rev. B* 101, 094506 (2020).
- [44] O. L. T de Menezes and J.S Helman, Spin flip enhancement at resonant transmission, *Am. J. Phys* 53, 1100 (1985).
- [45] H. D. Liu, X. X. Yi, Geometric phases in a scattering process, *Phys. Rev. A* 84, 022114 (2011).

- [46] G. Cordourier-Maruri, Y. Omar, R. de Coss, and S. Bose, Graphene-enabled low-control quantum gates between static and mobile spins, *Phys. Rev. B* 89, 075426 (2014).
- [47] F. Ciccarello, G. M. Palma, and M. Zarcone, Entanglement-induced electron coherence in a mesoscopic ring with two magnetic impurities, *Phys. Rev. B* 75, 205415 (2007).
- [48] S. Pal and C. Benjamin, Yu-Shiba-Rusinov bound states induced by a spin flipper in the vicinity of a s-wave superconductor, *Sci. Rep.* 8, 11949 (2018).
- [49] F. Setiawan, P. M. R. Brydon, J. D. Sau and S. DasSarma, Conductance spectroscopy of topological superconductor wire junctions, *Phys. Rev. B* 91, 214513 (2015).
- [50] A. Furusaki, & M. Tsukuda, Dc Josephson effect and Andreev reflection, *Solid state Commun.* 78, 299 (1991).
- [51] H. Enoksen, J. Linder, & A. Sudbø, Spin-flip scattering and critical currents in ballistic half-metallic d-wave Josephson junctions, *Phys. Rev. B* 85, 014512 (2012).
- [52] G. Annuziata, H. Enoksen, J. Linder, M. cuoco, C. Noce and A. Sudbo, Josephson effect in S/F/S junctions: Spin bandwidth asymmetry versus Stoner exchange, *Phys. Rev. B* 83, 144520 (2011).
- [53] A. A. Golubov, M. Y. Kupriyanov, & E. Il'ichev, The current-phase relation in Josephson junctions, *Rev. Mod. Phys.* 76, 411 (2004).
- [54] W. L. McMillan, Theory of Superconductor-Normal-Metal Interfaces, *Phys. Rev.* 175, 559 (1968).
- [55] J. Cayao and A. M. Black-Schaffer, Odd-frequency superconducting pairing and subgap density of states at the edge of a two-dimensional topological insulator without magnetism, *Phys. Rev. B* 96, 155426 (2017).
- [56] J. Cayao and A. M. Black-Schaffer, Odd-frequency superconducting pairing in junctions with Rashba spin-orbit coupling, *Phys. Rev. B* 98, 075425 (2018).
- [57] A. G. Lebed, Revival of superconductivity in high magnetic fields and a possible p -wave pairing in $(\text{TMTSF})_2\text{PF}_6$, *Phys. Rev. B* 59, R721(R) (1999).
- [58] I. J. Lee et al., Triplet Superconductivity in an Organic Superconductor Probed by NMR Knight Shift, *Phys. Rev. Lett.* 88, 017004 (2001).
- [59] W. Wernsdorfer et al., Spin-parity dependent tunneling of magnetization in single-molecule magnets, *Phys. Rev. B* 65, 180403(R) (2002).